

Preliminary Title:

Plasma Wakefield Acceleration

Veronica K. Berglyd Olsen
Department of Physics
University of Oslo
Norway



Dissertation Presented for the Degree of
Philosophiae Doctor (PhD) in Physics

July 2017

Abstract

Abstract

Acknowledgements

Acknowledgements

Contents

Preface	1
1 Introduction	3
1.1 Plasma Wakefield Acceleration	3
1.1.1 Laser Driven Acceleration	4
1.1.2 Beam Driven Acceleration	5
1.2 Beam-Plasma Interaction	5
1.2.1 The Drive Beam	5
1.2.2 The Linear Regime	7
1.2.3 The Non-Linear Regime	8
1.2.4 Beam Matching	8
1.3 Protons vs. Electrons as Drive Beam	9
1.4 The Self-modulation Instability	9
1.5 Numerical Simulations of PWFA	9
2 A Wakefield Accelerator Experiment	11
2.1 Evolution of the Concept	12
2.2 AWAKE: A Design Overview	12
2.2.1 Plasma Source	12
2.2.2 Electron Source	13
2.3 Stages of the Experiment	14
2.3.1 AWAKE Run 1	14
2.3.2 AWAKE Run 2	14
2.4 The Self-modulation Instability in AWAKE	15
3 Simulations	17
3.1 Evolution of the Proton Beam	17
3.1.1 Studies with Pre-modulated Beam	18
3.1.2 Studies with Single Drive Bunch	18
3.2 Beam Loading and Energy Spread	18
3.2.1 The Linear Regime	18
3.2.2 The Quasi-linear Regime	18
3.3 Emittance Evolution	18
3.3.1 The Quasi-linear + Non-Linear Case	19
3.4 Optimising the Witness Beam	19

Contents

4 AWAKE Data Acquisition	21
4.1 Experiment Setup	21
4.2 Data Acquisition	21
4.2.1 Front End Software Architecture (FESA)	21
4.2.2 AWAKE Integration: File Readers	21
5 Summary and Conclusion	23

Publications

I Loading of a Plasma-Wakefield Accelerator Section Driven by a Self-Modulated Proton Bunch, <i>Proceedings of IPAC 2015</i>	27
II Loading of Wakefields in a Plasma Accelerator Section Driven by a Self-Modulated Proton Beam, <i>Proceedings of NAPAC 2016</i>	33
III Data Acquisition and Controls Integration of the AWAKE Experiment at CERN, <i>Proceedings of IPAC 2017</i>	39
IV Emittance Preservation of an Electron Beam in a Loaded Quasi-Linear Plasma Wakefield, <i>Physical Review Accelerators and Beams</i>	45

Appendices

A Particle in Cell (PIC)	57
A.1 Full PIC	57
A.2 Quasi-Static PIC	57
A.3 Numerical Cherenkov	57
B Data Analysis	59
B.1 Osiris Analysis Toolbox	59
B.1.1 OsirisAnalysis Core Objects	60
B.1.2 OsirisAnalysis Data Types	60
B.1.3 OsirisAnalysis Graphical Interface and Plots	61
B.2 QuickPIC Analysis Framework	61
Bibliography	63

Preface

The work presented in this thesis is aimed towards addressing some of the questions surrounding the design of Run 2 of the AWAKE experiment at CERN (see Chapters 1 and 2). It is published in the following four papers:

- I Loading of a Plasma-Wakefield Accelerator Section Driven by a Self-Modulated Proton Bunch, *Proceedings of IPAC 2015* [11]
- II Loading of Wakefields in a Plasma Accelerator Section Driven by a Self-Modulated Proton Beam, *Proceedings of NAPAC 2016* [12]
- III Data Acquisition and Controls Integration of the AWAKE Experiment at CERN, *Proceedings of IPAC 2017* [13]
- IV Emittance Preservation of an Electron Beam in a Loaded Quasi-Linear Plasma Wakefield, *Physical Review Accelerators and Beams* [?]

The thesis also includes an introductory chapter outlining some of the core concepts involved in plasma wakefield acceleration techniques in Chapter 1. The AWAKE experiment itself is outlined in more detail in Chapter 2. The simulations forming the basis for the publications are described in Chapter 3, where the approximations used are also described. In Chapter 4 some of the additional work of integrating the AWAKE experiment with the CERN Control System is outlined. A final summary and conclusions are found in Chapter 5.

The four publications are included in this thesis in an appendix titled Publications. Additional appendices outlining the principles of Particle in Cell codes used in this work, and the analysis code written, are also included.

Notation

Table 1: Overview of notation used in this thesis.

Notation	Description
n_0	The average or initial plasma density
n_{pe}	The density of plasma electrons
n_b	The density of a general particle beam
n_{eb}, n_{pb}	The density of an electron or a proton beam in particular
σ_r	The width of a Gaussian beam when it is assumed to be round
σ_x, σ_y	The transverse size of a Gaussian beam when it may not be round, or the value applies to only one plane.
α, β, γ	The Twiss parameters, also known as the Courant-Snyder parameters [25].
β_r, γ_r	Relativistic factors*

- * These are indexed with r in this thesis to separate them from the Twiss parameters.

1

Introduction

The Advanced Wakefield Experiment (AWAKE) [8], located at the old CNGS¹ facility at CERN, became operational in December 2016. It is a proof-of-concept Proton Driven Plasma Wakefield Accelerator (PDPWFA) using the proton beam from the Super Proton Synchrotron (SPS) as its drive beam.

AWAKE is currently in Run 1 where the interaction between the proton drive beam and the plasma will be studied, and where a long electron witness beam will be injected to sample the wakefields. Run 2 is planned to start after the next Long Shutdown of the LHC (LS2) scheduled for 2019 and 2020, when significant upgrades will be made to the experiment. Run 2 will attempt to accelerate a short, intense electron beam to high energy while avoiding growth in emittance and large energy spread. In preparation for Run 2, a number of design choices needs to be made based on the results of Run 1 as well as simulations of Run 2. The work presented in this thesis primarily focuses on the beam loading of a short electron witness beam through simulations, in preparation for AWAKE Run 2.

The key results are presented in Publication IV, with the studies leading up to this presented in two conference papers: Publication I and II. A third conference paper, Publication III, covers the integration of the AWAKE experiment with the CERN control system, which is the main contribution to Run 1 in this PhD project.

In this chapter we will first cover some of the key concepts involved in plasma wakefield acceleration techniques relevant to the work presented in this thesis. The design of the AWAKE experiment itself is laid out in more detail in the next chapter, and the framework for the simulations is described in the third chapter. The fourth chapter outlines the work done in integrating AWAKE Run 1 with the control system at CERN.

1.1 Plasma Wakefield Acceleration

Accelerating particle beams in a plasma is an attractive concept as plasmas are capable of sustaining significantly higher accelerating fields than RF structures used in conventional accelerators can. Such RF structures suffer electrical breakdowns at very high electric fields, and these breakdowns can over time damage the structures [16]. This puts an upper limit on the accelerating gradient of about 350 to 400 MV/m. As these breakdowns causes damage to the surfaces of the RF cavities, in practice the upper limit is determined by the statistical probability of a

¹The CERN Neutrinos to Gran Sasso (CNGS) experiment was operational between 2006 and 2012.

breakdown and the acceptable number of breakdowns in a given period of time [60], and the practical limit is therefore lower.

While RF cavities use standing electromagnetic waves to accelerate particles, plasma accelerators use an energetic beam to drive strong electromagnetic wakefields in the plasma. The two main techniques for producing these strong accelerating fields are by the use of an intense laser beam, or by the use of a particle drive beam. Laser accelerator techniques were investigated in the early 1970s [20, 57], and wakefield acceleration techniques through the use of computer simulations at the end of the decade [67]. Using particle beams to drive accelerating wakefields were proposed some time later, in 1985 [22].

Both these beam and laser driver techniques utilise a neutral plasma where the collective motion of the free electrons define the main parameters of the accelerating structure. The characteristic time of the electron motion is related to the plasma frequency, ω_{pe} , and the characteristic length is related to the plasma wavelength, λ_{pe} .

$$\lambda_{pe} = \frac{2\pi c}{\omega_{pe}}, \quad \omega_{pe} = \sqrt{\frac{n_0 e^2}{m_e \epsilon_0}}, \quad (1.1)$$

where n_0 is the initial plasma electron density, e is the elementary charge, m_e is the electron mass, and ϵ_0 is the vacuum permittivity [28, 58, 68]. Here we ignore the ion mass and we assume the plasma is cold, i.e. we ignore the thermal motion of the electrons. The characteristic time and length of ion motion scales as the square root of the mass difference compared to the plasma electrons and tend, depending on the ion mass, to be a few orders of magnitude longer than those of the electrons. In the case of very long accelerating structures, the motion of the ions may become an issue.

Plasmas can in general sustain accelerating electric fields on the order of the non-relativistic wave-breaking field [26, 28]

$$E_{WB} = \frac{m_e c \omega_{pe}}{e}. \quad (1.2)$$

For instance, for a plasma density of 10^{18} cm^{-3} , the maximum field is on the order of 100 GV/m . This has been inferred by experiment in the mid 1990s when a few electrons was accelerated to over 40 MeV in about $300 \mu\text{m}$ of Helium plasma, driven by a 25 TW pico second laser [51].

Both techniques require a drive beam that deposits energy into the plasma in the form of wakefields. The drive beam is trailed by another beam which draws energy from the fields in order to accelerate. We thus see a transfer of energy from the drive beam to the witness beam through plasma as the intermediate medium [53]. Let us briefly introduce the core principle of the two methods of plasma wakefield acceleration.

1.1.1 Laser Driven Acceleration

In a laser wakefield driven plasma accelerator (LWFA), the plasma acts like a transformer, changing high frequency transverse field of the laser pulse into a low frequency longitudinal wave [49]. The effect driving the accelerating fields was described by Tajima and Dawson in 1979, and can be summarised as follows: The ponderomotive force at the front of the laser pulse drives plasma electrons forward, while at the back of the pulse it pushes them backwards. This generates a longitudinal wave that is at its most efficient when the length of the laser

pulse $L_{ph} = \lambda_{pe}/2$ [67]. The longitudinal field is then loaded by a trailing particle beam to be accelerated, or in some instances plasma electrons are being captured and accelerated instead.

1.1.2 Beam Driven Acceleration

In a beam driven plasma wakefield acceleration (PWFA) a drive beam of charged particles are sent through a section of neutral plasma. The space charge of the drive beam displaces the plasma electrons, which oscillate at the plasma frequency, creating periodic regions of low and high electron density generating strong wakefields. The longitudinal and transverse fields generated by this wake is then loaded by a trailing beam of particles. The principles behind this technique were formulated in the 1980s by Pisin Chen *et al.* [22].

Any type of charged particle beam can be used in such an accelerator. Most experiments to date have used electrons. It has been shown that energy can be transferred from one or more electron drive beams to a single electron witness beam in multiple past experiments [15, 38, 45, 63]. In one experiment at the Stanford Linear Accelerator Center (SLAC), a 42 GeV electron beam passing through an 85 cm section of ionised Lithium vapour, saw the trailing part of the electron beam reach 85 GeV. This corresponds to a gradient of 52 GV/m [15].

A limitation using an electron beam with a similar initial charge and energy for both drive and witness beams is that the witness beam will rapidly gain energy, while the drive beam loses energy. This both causes the drive beam to quickly decelerate, while the witness beam undergoing acceleration will at the same time catch up with the drive beam. Typically propagation length of an electron drive beam is a few tens of centimetres of plasma.

1.2 Beam-Plasma Interaction

As a relativistic, charged beam propagates through plasma, it affects the local density of the plasma electrons. The charged beam generates strong transverse fields, pushing or pulling the plasma electrons away or towards the propagation axis of the beam [2, 43]. As the heavier plasma ions will move on a much longer time scale, due to inertia, the plasma electrons expelled from the axis will be pulled back towards it by the ion charge. The electrons will tend to overshoot the axis, creating an oscillation system. A positively charged drive beam will initially pull the electrons towards the axis, where they overshoot, creating a similar effect to a negative drive beam with a half-period phase offset. The oscillation period is determined by the plasma wavelength of the electrons [36, 52]. An illustration of an electron beam travelling though a plasma is shown in Figure 1.1.

1.2.1 The Drive Beam

The wakefields generated by a charged drive beam are given by the Lorentz force

$$\vec{W} = \frac{\vec{F}}{q_b} = \vec{E} + \vec{v}_b \times \vec{B}, \quad (1.3)$$

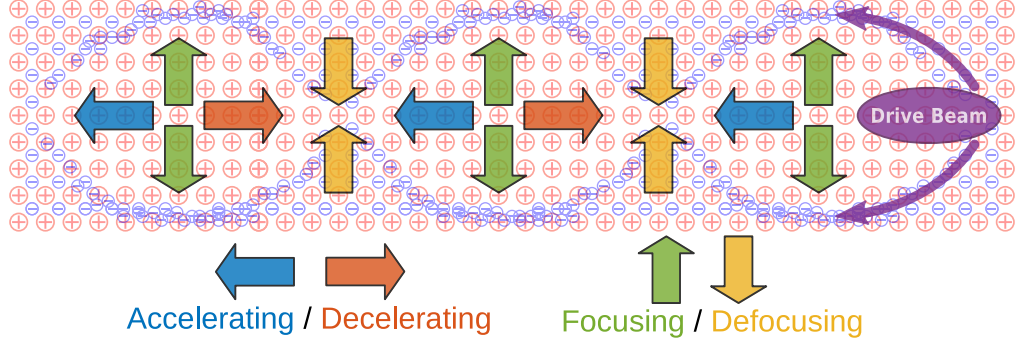


Figure 1.1: Illustration of a plasma wakefield accelerating structure with a single electron drive beam. A series of focusing/defocusing and accelerating/decelerating regions (as seen for an electron witness beam) are produced behind the drive beam.

where q_b is the beam charge and \vec{v}_b is the beam velocity. We define the longitudinal coordinate in the frame of the beam along its direction of propagation as

$$\xi \equiv z - v_b t \approx z - ct, \quad (1.4)$$

and for the purpose of the following derivations, we use a cylindrical coordinate system (r, ξ) . It follows, then, that the longitudinal wakefield is only determined by the longitudinal component of the electric field – to the first order – such that

$$W_{\parallel}(r, \xi) = E_z(r, \xi). \quad (1.5)$$

The transverse wakefield, on the other hand, also depends on the magnetic field such that

$$W_{\perp}(r, \xi) = E_r(r, \xi) - cB_{\theta}(r, \xi), \quad (1.6)$$

where we again take the velocity of the beam to be $v_b \approx c$.

A charged beam will diverge and lengthen due to space charge, but since the beam is relativistic the effect is of no significance over a few metres of plasma. Dephasing ΔL over a distance L can be estimated as

$$\frac{\Delta L}{L} \approx \frac{1}{\gamma^2} \frac{\Delta \gamma}{\gamma} \quad (1.7)$$

for two sample particles with energy difference $\Delta \gamma$ [52]. In the transverse plane, however, the beam is subject to the Lorentz force given by the transverse component of Eq. 1.3. Taking Maxwell's equations and $B_{\theta} = v_b E_r / c^2$ [65], the strength can be estimated using an infinitely long, uniform beam of density n_b :

$$F_{\perp} = q_b(E_r - v_b B_{\theta}) = q_b E_r \left(1 - \frac{v_b^2}{c^2}\right) = \frac{1}{\gamma^2} q_b E_r. \quad (1.8)$$

The implication being that for relativistic beams, the transverse dynamics are dominated by emittance and external forces [52].

1.2.2 The Linear Regime

When the charge density of the beam is smaller than that of the plasma, $n_b \ll n_{pe}$, the system is in the *linear regime*. The linear regime is not of much interest for accelerator applications as it does not produce strong wakefields, and the transverse and longitudinal fields have continuous variations. These variations will strongly affect the energy spread and emittance of the witness beam. However, this regime is interesting from a theoretical perspective because it is well described analytically [52].

A linear theory for plasma accelerators can be derived using a cold, non-relativistic fluid model of the plasma. The response of the cold plasma can be found from the linearised equations of motion and continuity, and the Maxwell equations. (For examples of linearisation, see [21, 58].) The equations of motion and continuity are linearised assuming the perturbed plasma density, n_1 , is much smaller than the unperturbed density, $n_0 = n_{pe}$ [23]. By further combining the fluid equation and the Poisson equation [39], a wave equation for the plasma density perturbation by the beam can be derived [23, 52]:

$$\frac{\partial^2}{\partial \xi^2} n_1 + k_{pe}^2 n_1 = \frac{q_b}{e} k_{pe}^2 n_b, \quad (1.9)$$

where we still assume $n_b \ll n_{pe}$.

The solution to Eq. 1.9 in the longitudinal dimension is the Green's function for a harmonic oscillator in 1D [39], and the radial dependency can be calculated from 2D theory for different radial profiles [23]. For a beam that has a Gaussian profile in both dimensions, the wakefields are

$$W_{\parallel}(r, \xi) = \frac{e}{\epsilon_0} \int_{-\infty}^{\xi} n_{b\parallel}(\xi') \cos [k_{pe}(\xi - \xi')] d\xi' \cdot R(r) \quad (1.10)$$

$$W_{\perp}(r, \xi) = \frac{e}{\epsilon_0 k_{pe}} \int_{-\infty}^{\xi} n_{b\parallel}(\xi') \sin [k_{pe}(\xi - \xi')] d\xi' \cdot \frac{d}{dr} R(r), \quad (1.11)$$

where the transverse dependency $R(r)$ is

$$R(r) = k_{pe}^2 \int_0^r n_{b\perp}(r') I_0(k_{pe} r') K_0(k_{pe} r) r' dr' \\ + k_{pe}^2 \int_r^{\infty} n_{b\perp}(r') I_0(k_{pe} r) K_0(k_{pe} r') r' dr'. \quad (1.12)$$

Here I_0 and K_0 are the zeroth-order modified Bessel functions of the first and second kind, respectively [23, 52].

As can be seen from Figure 1.2, the longitudinal wakefield is at its maximum on-axis. For very wide beams, $\sigma_r \gg k_{pe}$, we converge at the 1D result as we expect. For very narrow beams, $\sigma_r \gg k_{pe}$, the maximum decreases rapidly with radius causing different parts of the witness beam at different radii to see different accelerating fields. The cosine component of Eq. 1.10 also implies longitudinal variations of the accelerating field. Combined, these produce a large energy spread for the accelerating beam. Additional, the sinusoidally varying focusing field from Eq. 1.11 produces emittance growth [39, 52].

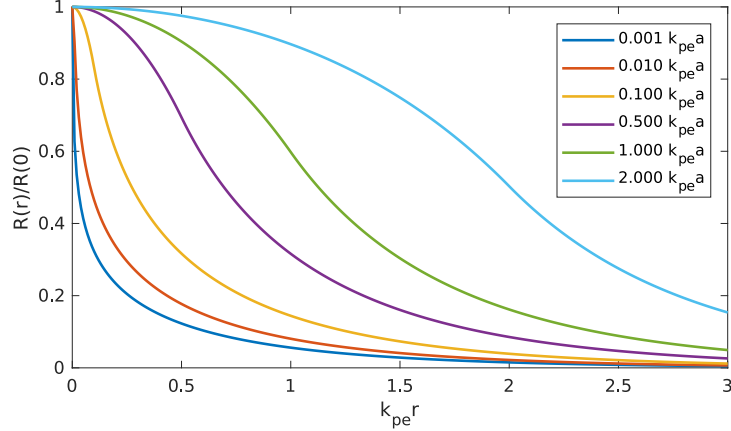


Figure 1.2: The radial function $R(r)$ for a range of uniform beams cut off at a radius a up to twice the plasma skin depth k_{pe} . The plot is reproduced from Katsouleas *et al.* [39].

1.2.3 The Non-Linear Regime

In the non-linear regime, also referred to as the *blowout* regime in the literature, the plasma electrons are expelled from the region around the axis to form a region populated by only plasma ions. As the ions are practically stationary on the time scale of the plasma electrons, they form a uniform column of positive charge. The electrons displaced by the space charge of the drive beam are pulled back on axis by the ions, within the characteristic time ω_{pe}^{-1} , to form a thin sheath of electrons with the shape of a bubble [47, 48]. Hence, this is also sometimes referred to as the *bubble* regime or the *blow out* regime.

A conceptual illustration of an electron beam driven plasma accelerator is shown in Fig. 1.1. Several regions of decreasing magnitude of accelerating/decelerating and focusing/defocusing are generated behind the drive beam. By positioning a trailing beam in an optimal phase, such a beam can both accelerate and focus. The drive beam needs to be shorter than the plasma period for this structure to develop, but multiple short drive beams with a separation of the plasma wave length can amplify the wakefields.

1.2.4 Beam Matching

In the non-linear case where an ion column is formed, the focusing force it produces will cause a pinching effect on the beam. The beam itself, assuming $\epsilon_N > 0$, will cause the beam to try to expand. There exists a beam radius where the focusing force and the beam's tendency to expand are in equilibrium. For a highly relativistic beam, $\gamma_r \gg 1$, the equilibrium radius is given by [40]

$$R_{eq} = \left(8 \frac{\epsilon_N^2 c^2}{\gamma_r \omega_p^2} \right)^{1/4}. \quad (1.13)$$

Equation 1.13 follows from the general envelope equation [42] under the assumption that the beam enters the plasma at focus (i.e. $d\sigma_r / dz = 0$), does not diverge significantly from a Gaussian transverse density profile, and that the focusing force is linear [40] – the latter being the case in the blow-out regime.

1.3 Protons vs. Electrons as Drive Beam

Further details on proton driven plasma wakefield goes here.

Benefit of larger energy per bunch, challenge of producing short bunches.

Cite [1].

1.4 The Self-modulation Instability

A long beam with respect to the plasma wavelength will generate a density wave driven by its own head. This is true for both laser beams [27] and particle beams [41], and they are caused by the same underlying physics. For a laser beam, this produces alternating regions of focusing and diffraction. For a particle beam, the wakefields generated within the beam acts back on itself, breaking it up into short micro bunches with a surrounding, defocused halo.

In the 1980s, this self-modulating effect was taken advantage of in LWFA experiments as only long laser pulses were available. Advances in ultra short laser technology later removed the dependence of this effect [61], however for proton drive beams this is still an issue. For instance, the SPS proton beam used by AWAKE is orders of magnitude longer than the plasma wavelength needed for the experiment.

The self-modulation instability (SMI), is one of several instabilities affecting long beams in plasma.

In electron beam [54].

1.5 Numerical Simulations of PWFA

PIC codes. Osiris vs, QuickPIC.

Numerical Cherenkov, Lehe. Relevance to emittance.

Reference to PIC appendix.

Maybe something about resolution and convergence.

2 A Wakefield Accelerator Experiment

AWAKE is the first proton driven wakefield accelerator experiment in the world. It is a proof-of-concept experiment aiming to inform a design for future high energy accelerators [35]. The proton drive beam is delivered by the Super Proton Synchrotron (SPS) at CERN. The experiment is physically located at the former site of the CERN Neutrinos to Gran Sasso experiment (CNGS) [33], in a tunnel below the Swiss-French border, connected to the SPS at SPS Point 4. The placement of the AWAKE experiment in relation to the rest of the CERN accelerator complex can be seen in Figure 2.1.

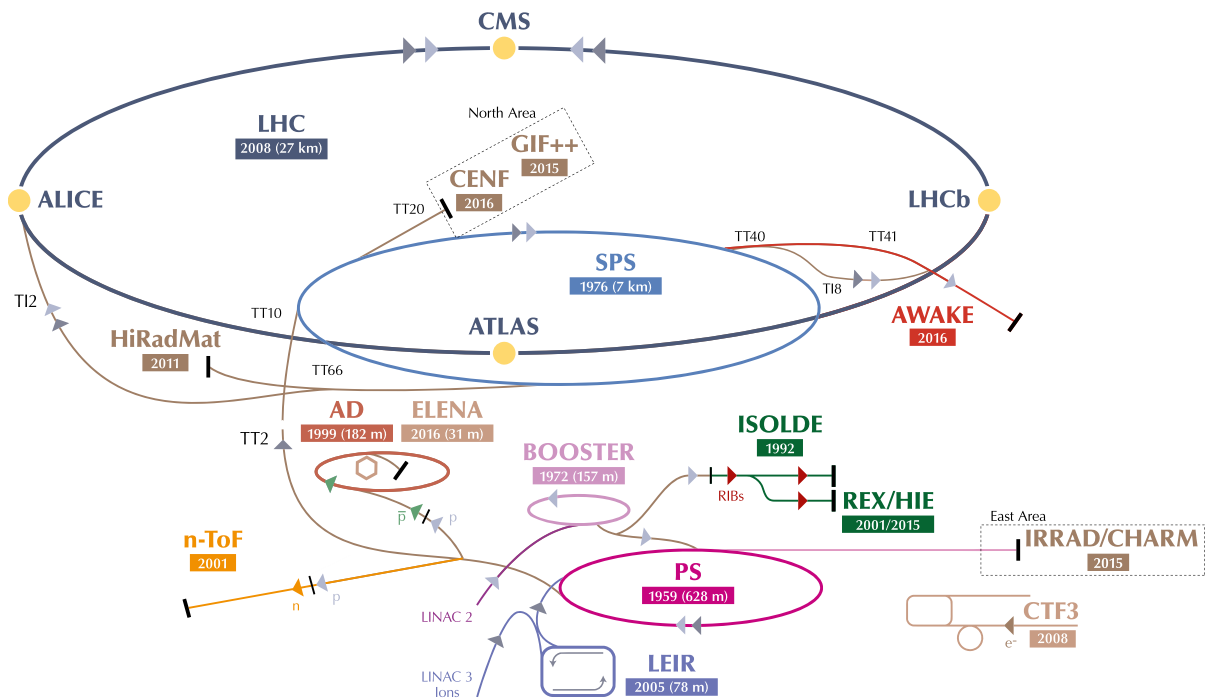


Figure 2.1: An overview of the CERN Accelerator Complex [50].

Intro paper [17]

Launch paper [8]

Evolution paper [19]

Technical specs including simulation parameters [35]

Collaboration paper by Patric [55]

2.1 Evolution of the Concept

Previous experiments, SLAC, etc.

[15, 38, 45, 63]

Self modulation at FACET [3]

Review by Patric [53]

2.2 AWAKE: A Design Overview

AWAKE is, as of the writing of this thesis, operational and in Run 1. The proton beam line arriving from the SPS joins with the laser beam, and the electron beam line, and connects to a 10 m plasma stage. In addition, an electron source has been installed, and a new side tunnel had to be dug to fit the electron beam line connecting the source to the main assembly. Figure 2.2 gives an overview of the experimental layout in the tunnel. The old CNGS target is still present, behind a shielding wall as it is highly radioactive. This, unfortunately, has created some constraints for fitting the downstream beam line and diagnostics, and may pose additional challenges for Run 2.

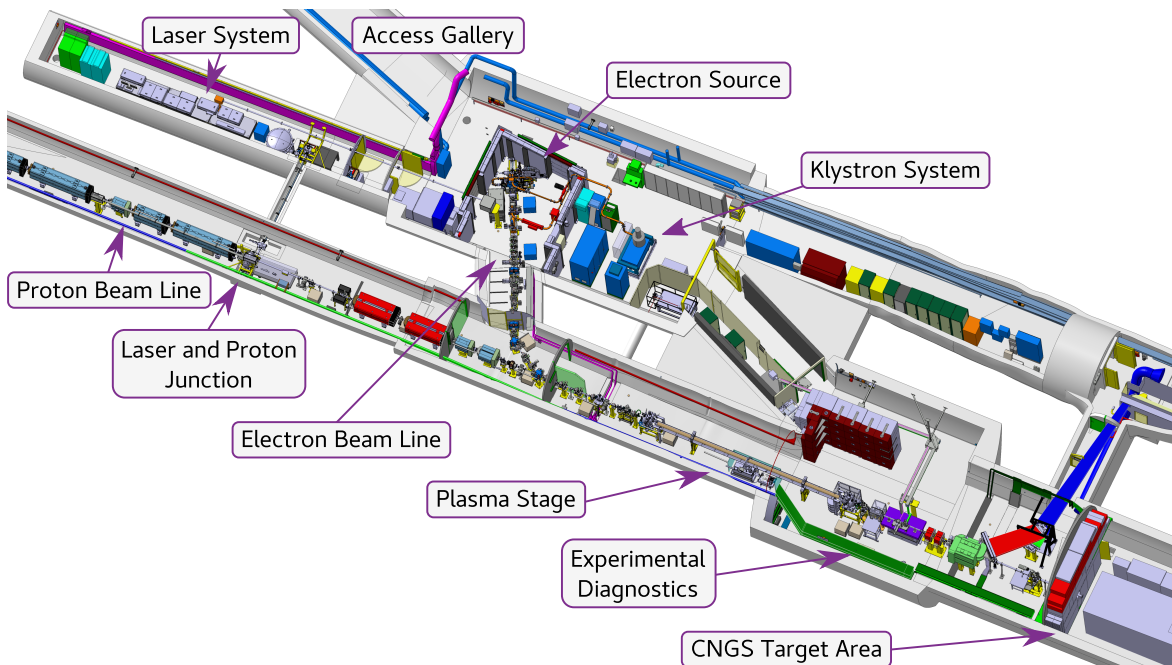


Figure 2.2: Drawing of the AWAKE experimental area with the key components labelled.

2.2.1 Plasma Source

The requirements for the plasma source for AWAKE Run 1 were a 10 m long cell with a plasma electron density range of $1 - 10 \times 10^{14} \text{ cm}^{-3}$. The density variation should be within 0.2%, and the radius of the plasma channel should be $\geq 1 \text{ mm}$. The plasma should also consist of heavy ions to mitigate ion motion [18].

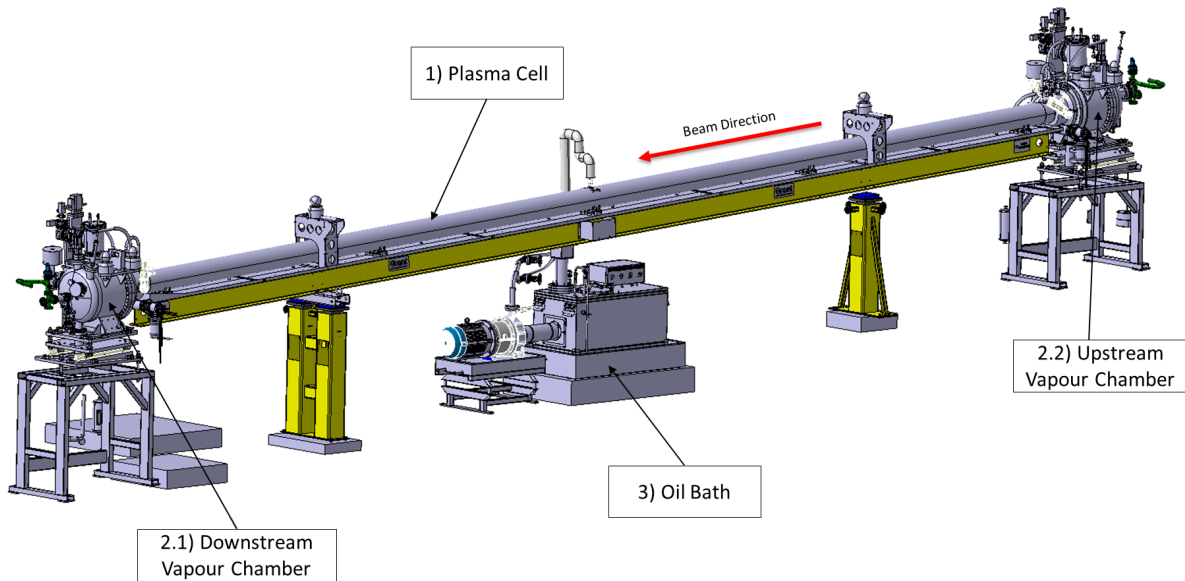


Figure 2.3: A CAD drawing of the plasma cell and its related components, as presented in the 2016 AWAKE Status Report [6].

For the AWAKE vapour source, rubidium (Rb) was chosen. Rubidium has a low melting point, 39.3 °C; a low first ionisation energy, 4.18 eV; and a standard atomic weight of 85.47. The plasma wavelength of rubidium ions with a +1 charge is roughly 400 times that of the plasma electrons (see Eq. 1.1), preventing significant ion motion for AWAKE application [70]. An additional benefit of using an alkaline metal like rubidium is that the second ionisation level is significantly higher, 27.3 eV, making it relatively easy to prevent further ionisation and thus a lower charge/mass ratio [7]. The rubidium vapour is created by heating the reservoir and the plasma cell to around 150 – 230 °C to reach the density range required for AWAKE [18, 55].

The ionisation of the Rb vapour is achieved with a short laser pulse co-propagating with the proton drive beam. The laser can be timed such that the plasma channel is created inside the beam itself. The short laser pulse produces a sharp plasma edge that provides a good seed for the self-modulation instability [71]. The section of the proton beam ahead of the laser does not interact strongly with the neutral rubidium vapour, although a low level of impact ionisation does occur. However, this effect is not significant [7].

The ionisation laser used for AWAKE is a 780 nm Ti:Sapphire laser with a pulse length of 120 fs and a maximum compressed energy of 450 mJ. The peak intensity is around $1.2 \times 10^{14} \text{ W/cm}^2$, with a spot size radius of 1 mm [7]. The appearance intensity needed for ionisation of rubidium is around $1.7 \times 10^{12} \text{ W/cm}^2$ [5]. Ionisation of a second electron requires some 455 times higher intensity, so we expect no secondary ionisation [55].

2.2.2 Electron Source

The AWAKE electron source needed for Run 1 consists of a 2.5 cell RF-gun and a 1 m long booster structure, both operating at 3 GHz, a cathode transfer chamber, beam diagnostics, and a beam transport line connecting it to the proton beam line. The beam is boosted to up to 20 MeV by a constant gradient acceleration structure. The RF-gun and the booster are powered by a

30 MW klystron [7, 59]. Several of the components, including the RF-gun and klystron, were re-purposed from the former PHIN injector in the CLIC test facility [24]. An overview of the electron source and the accelerating structure can be seen in Figure 2.4.

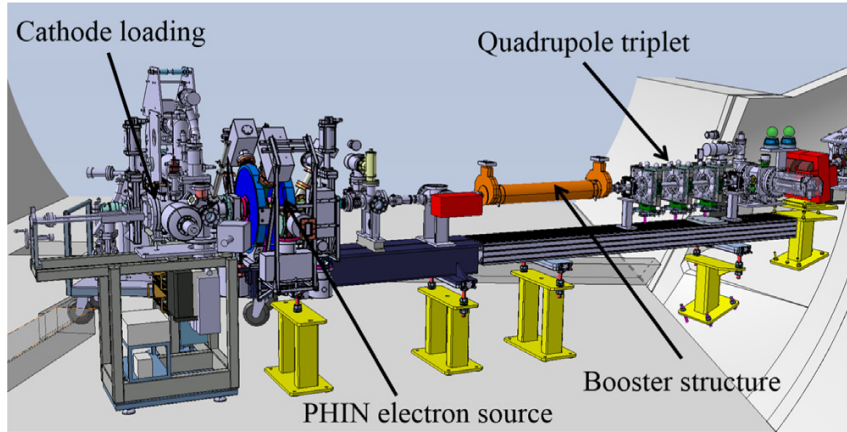


Figure 2.4: A CAD drawing of the electron source and accelerating structure [59].

2.3 Stages of the Experiment

A summary of the AWAKE experiment

2.3.1 AWAKE Run 1

Table 2.1: Nominal AWAKE experiment beam parameters for Run 1 [34, 35].

Parameter	Proton Beam	Electron Beam
Momentum	400 GeV	16 MeV
Charge	4.8 nC	200 pC
Particles	3×10^{11}	1.25×10^9
Bunch length (σ_z)	12 cm (0.4 ns)	1.2 mm (4 ps)
Bunch size ($\sigma_{x,y}$)	200 μm	250 μm
Normalised emittance (ϵ_N)	3.5 μm	2 μm
Relative energy spread ($\Delta p/p$)	0.035%	0.5%
Beta function ($\beta_{x,y}^*$)	4.9 m	0.4 m
Dispersion ($D_{x,y}^*$)	0	0

Description of Run 1. SMI, long e-beam.

2.3.2 AWAKE Run 2

Short e-beam, multiple stages, etc.

Problems relevant for this thesis.

Erik [1]

2.4 The Self-modulation Instability in AWAKE

Results from Run 1 of the experiment.

Karl [62]

Does the SMI require a seed? See muggli:2017 [55].

3 Simulations

The work presented in this thesis has been done using simulations with two particle-in-cell (PIC) codes; OSIRIS [30] and QuickPIC [4, 37]. OSIRIS is a proprietary full PIC code available in 1, 2 and 3 dimensions, with a choice between cartesian and cylindrical coordinates. QuickPIC is a quasi-static 3D PIC code. In this work the open source version of QuickPIC has been used [69]. For a more detailed description on PIC codes, see Appendix A.

Although PIC codes use macro particles, that is, simulated particles represent more than one physical beam or plasma particle, these codes require a lot of CPU power. This is especially true when running in 3D. The preliminary studies presented in Publications I and II were done using OSIRIS with 2D cylindrical coordinates. The main study, Publication IV, was done using QuickPIC in 3D. In order to perform the detailed parameter scans needed for these studies, the drive beam and accelerating structure had to be scaled down into a more manageable size than the full SPS proton beam. This section will outline the simulation environment chosen for these studies, and the reasons behind these.

3.1 Evolution of the Proton Beam

An initial set of simulations were run to study the evolution of the self-modulation instability in the SPS proton beam. These simulations assumed the plasma was ionised at the centre of the beam, so only the back half of the beam was actually simulated. The beam profile function took the form:

$$f(\xi, r) = \frac{A}{2} \left[1 + \cos \left(\xi \frac{\pi}{L} \right) \right] \exp \left(-\frac{r^2}{2\sigma_r^2} \right), \quad (3.1)$$

where $L = 2.5\sigma_{z,pb} = 30$ cm is the length of half an SPS proton bunch, R is the radius of the simulation box, and A_q is a charge scaling factor to match the SPS bunch charge. The charge of the proton beam in cylindrical coordinates is thus given by

$$Q_{pb} = 2\pi \iint f(\xi, r) r \, dr \, d\xi, \quad (3.2)$$

and A is tuned so that Q_{pb} matches the charge outlined in Table 2.1.

3.1.1 Studies with Pre-modulated Beam

In order to make the simulations more manageable in size, for the beam loading studies we decided to move to a sample proton beam of 26 micro bunches. The simulations were all done using OSIRIS 3.0. With this version it is necessary for the beams to drift in vacuum for a short distance for the EM-fields to develop properly as they start at zero (see further discussion in Section A.1). Since the evolution of the self-modulation instability was not of primary interest in this study, we chose to modify the beam profile to emulate a section of modulated beam. We refer to this as pre-modulation. This was done by shortening the wavelength of the profile in Eq. 3.1 to match that of the plasma wavelength:

$$f(\xi, r) = A\sqrt{2} \left[\frac{1}{2\sqrt{2}} + \cos(k_{pe}\xi - \mu) \right] \exp\left(-\frac{r^2}{2\sigma_r^2}\right), \quad (3.3)$$

where μ is the position of the first micro bunch and k_{pe} is the plasma wave number [11]. The offset of the cosine function is chosen such that the width of the micro bunch matches the width of a bunch in the simulations done with a full beam. Since OSIRIS ignores profile densities with negative values, the profile is automatically clipped at 0.

Due to the necessary initial drift stage of these simulations, it is technically challenging to inject an electron witness beam while strictly controlling parameters like emittance, energy spread and transverse size as these evolve during this drift phase. There are several ways of preventing the beam from evolving, like slowly ramping up the beam charge or ramping up the beam energy.

3.1.2 Studies with Single Drive Bunch

Text

3.2 Beam Loading and Energy Spread

Text

3.2.1 The Linear Regime

The ideal case from Tzoufras 2008.

3.2.2 The Quasi-linear Regime

Text

3.3 Emittance Evolution

Emittance is preserved in the linear regime

3.3.1 The Quasi-linear + Non-Linear Case

An electron beam matched to the typical AWAKE plasma density will be, as discussed in 1.2.4, very narrow. At a typical normalised emittance of $2.0 \mu\text{m}$ the beam is $5.25 \mu\text{m}$. Even at low beam charge and at the upper limit in terms of beam length, the wakefields of such a beam will quickly reach the non-linear regime. In the base case used in the beam loading study included in Publication IV [14] the peak density of the beam $n_b/n_0 > 35$, well beyond the saturation level of the bubble that occurs when $n_b/n_0 > 10$ [46].

The implication here is that there is an additional beneficial effect of loading the accelerating field with as much charge as it will allow without overloading it. The resulting non-linear wake driven by the head of the beam, which will see emittance growth due to the quasi-linear conditions of the proton wake, ensures that the rest of the beam sees a strong focusing force preventing further emittance growth. As the electron beam gains energy, its transverse size will decrease as its emittance is preserved as $\sigma_r = \sqrt{\epsilon_N \beta}$ [72].

3.4 Optimising the Witness Beam

Bringing it all together.

4 AWAKE Data Acquisition

Chapter introduction

4.1 Experiment Setup

Plasma density measurement [56]

Laser diagnostics [64]

Scopes

Universal class for probe measurements, etc.

4.2 Data Acquisition

Text

4.2.1 Front End Software Architecture (FESA)

The Front End Software Architecture (FESA), is a software framework originally developed at CERN. It provides a set of tools for developers to generate large portions of the code needed to control and read instruments and control infrastructure in the main accelerators at CERN. Collectively, the FESA classes provide a standard API towards the higher layers of the controls framework.

While originally developed by CERN, FESA was always intended to be usable for other experiments. The current iteration FESA3, is developed in collaboration with GSI Helmholtz Centre for Heavy Ion Research in Germany where it is used at the FAIR facility [66].

4.2.2 AWAKE Integration: File Readers

A summary of how the file reader classes have been designed. Flow chart from presentation. Describe the logic behind it and some of the challenges.

5 Summary and Conclusion

Text

Publications

Publication I

Loading of a Plasma-Wakefield Accelerator Section Driven by a Self-Modulated Proton Bunch

Abstract: We investigate beam loading of a plasma wake driven by a self-modulated proton beam using particle-in-cell simulations for phase III of the AWAKE project. We address the case of injection after the proton beam has already experienced self-modulation in a previous plasma. Optimal parameters for the injected electron bunch in terms of initial beam energy and beam charge density are investigated and evaluated in terms of witness bunch energy and energy spread. An approximate modulated proton beam is emulated in order to reduce computation time in these simulations.

Authors: Veronica K. Berglyd Olsen, Erik Adli (University of Oslo, Oslo, Norway), Patric Muggli (Max Planck Institute for Physics, Munich, Germany), Ligia D. Amorim, Jorge M. Vieira (Instituto Superior Technico, Lisbon, Portugal)

Publication: Proceedings of IPAC 2015, Richmond, Virginia, USA [[11](#)]

Date: 3rd to 8th of May, 2015

LOADING OF A PLASMA-WAKEFIELD ACCELERATOR SECTION DRIVEN BY A SELF-MODULATED PROTON BUNCH

V. K. Berglyd Olsen*, E. Adli (University of Oslo, Norway)

P. Muggli (Max Planck Institute for Physics, Munich, Germany)

L. D. Amorim, J. M. Vieira (Instituto Superior Technico, Lisbon, Portugal)

Abstract

We investigate beam loading of a plasma wake driven by a self-modulated proton beam using particle-in-cell simulations for phase III of the AWAKE project. We address the case of injection after the proton beam has already experienced self-modulation in a previous plasma. Optimal parameters for the injected electron bunch in terms of initial beam energy and beam charge density are investigated and evaluated in terms of witness bunch energy and energy spread. An approximate modulated proton beam is emulated in order to reduce computation time in these simulations.

INTRODUCTION

The AWAKE experiment [1] is a proof-of-principle demonstration of acceleration of an electron bunch to the TeV energy range in a single plasma section, using a proton bunch driver [2].

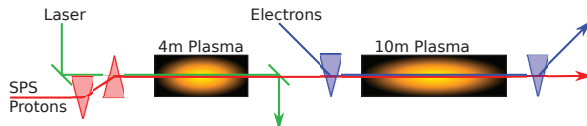


Figure 1: Simplified set-up of AWAKE Phase III. A long proton bunch experiences the SMI in a short plasma cell. The electron bunch is injected before the second plasma cell.

The AWAKE experiment proposes using a proton driver at 400 GeV, delivered by the SPS. The experiment is currently under construction at CERN, scheduled to start in late 2016. The SPS proton bunch is too long to generate a sufficiently strong wakefield [3]. A usable drive bunch needs to be close to the plasma wavelength λ_p in length; however, producing a short enough proton bunch is technically difficult.

The plasma wavelength and frequency are given by

$$\lambda_p = \frac{2\pi c}{\omega_p}, \quad \omega_p = \sqrt{\frac{N_p e^2}{m_e \epsilon_0}}, \quad (1)$$

where N_p is the plasma electron density, e is the elementary charge, m_e is the electron mass and ϵ_0 is the vacuum permittivity.

A proton bunch with $\sigma_{z,0} k_p \gg 1$, where $\sigma_{z,0}$ is the initial length of the bunch, will under certain conditions develop a self-modulation instability (SMI) when it travels through a plasma [4]. The proton bunch will then develop into a train of micro bunches with a period on the order of λ_p .

* v.k.olsen@fys.uio.no

3: Alternative Particle Sources and Acceleration Techniques

A22 - Plasma Wakefield Acceleration

In phase I of the AWAKE experiment the SMI of the proton bunch will be studied. In phase II, the proton wake will be studied using a long, externally injected electron bunch that will sample all phases of the wake. In phase III, acceleration of a short bunch in the wake of an already self-modulated proton beam will be studied, as illustrated in Fig. 1. In this paper we study the beam quality of a short electron bunch accelerated by an SMI proton wake in preparation for phase III of AWAKE.

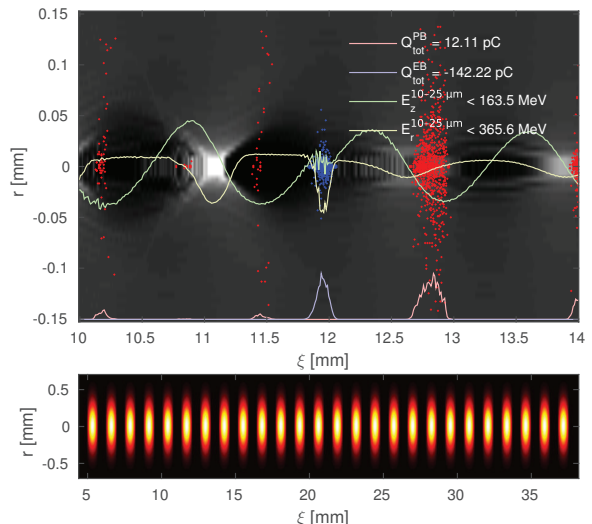


Figure 2: **Top:** An example showing the structure of the plasma electrons (grey) with a projection of the proton beam (red) and the electron bunch (blue) density on the bottom. The E_z (green) and E_r (yellow) fields have been overlaid on the plot. Shown is also a sample of electron (blue) and proton (red) macro particles. **Bottom:** An example of a pre-modulated proton drive beam at $t = 0$ plotted in terms of charge density.

SIMULATION SET-UP

All simulations in this paper have been performed using OSIRIS, a three-dimensional, relativistic, particle-in-cell code for modelling plasma based accelerators [5].

The parameter scans presented have all been run on a small scale test case with a shorter proton drive beam than AWAKE specifications. We simulate here only the second plasma stage in Fig. 1, assuming a pre-modulated proton beam profile with charge density function

$$\rho_{p^+}(\xi) = A \left[\frac{1}{2\sqrt{2}} + \cos(k_p \xi - \mu_1) \right] e^{-r^2/2\sigma_r}, \quad (2)$$

where A is a charge scaling factor, μ_1 is the centre position of the first micro bunch, $k_p = 2\pi\lambda_p^{-1}$ is the wave number, and $\xi = z - ct$ is the coordinates in a frame moving at the speed of light.

The length of the beam is limited by a step function to 33 mm. Negative density values for the density profile is ignored by OSIRIS. This gives a beam of 26 micro bunches of protons, as seen in the bottom plot of Fig. 2. The beam has a total initial charge of 2.6 nC, with an initial peak current per micro bunch of 135 A. For the proton beam $\sigma_r = 200 \mu\text{m} = 1.00 \text{ c}/\omega_p$ in all simulations, where c/ω_p is the plasma skin depth.

The electron witness bunch is injected between micro bunches 20 and 21 of the drive beam, at $\xi \approx 12 \text{ mm}$, see Fig. 2. The charge density of the electron bunch is given by

$$\rho_{e^-}(\xi) = Ae^{-(\xi-\mu)^2/2\sigma_z^2}e^{-r^2/2\sigma_r^2}. \quad (3)$$

For the electron bunch $\sigma_r = 105 \mu\text{m} = 0.52 \text{ c}/\omega_p$, and $\sigma_z = 40 \mu\text{m} = 0.2 \text{ c}/\omega_p$ in the cases with a short electron bunch. The plasma density at the beginning of the plasma section for all these simulations is $N_p = 7 \times 10^{14} \text{ cm}^{-3}$.

BEAM INJECTION

While the peak-to-peak distance between micro bunches of the self-modulated proton beam corresponds closely to the plasma wavelength λ_p , it is not constant along the length of the beam [6]. A brief study of the SMI of both full scale and small scale proton beams, using Fourier transform and Wavelet analysis, revealed that the fundamental frequency was slightly lower than one k_p .

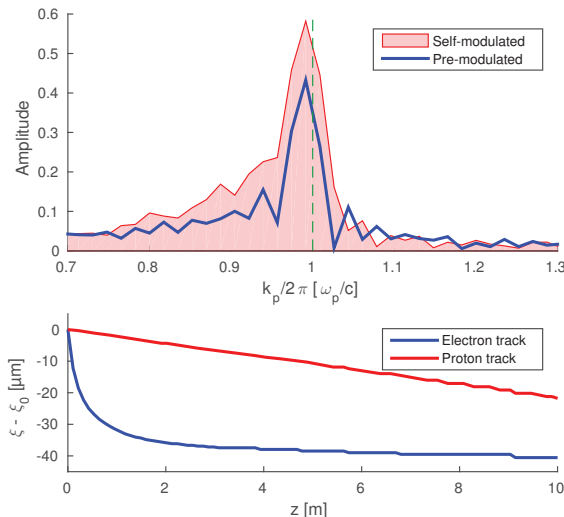


Figure 3: **Top:** The Fourier transform of the proton beam after 10 m of plasma for a self- and pre-modulated beam. The green line indicates $k_p = 2\pi/\lambda_p$. **Bottom:** Typical drift of a proton and electron macro particle through the plasma in respect to c .

To minimise further SMI development with a pre-modulated beam, the micro bunch distance was reduced

to $0.9939 k_p$, which produced a very good fit to the actual SMI for our test case, see Fig. 3.

An electron bunch of low MeV range initial energy will, due to its low gamma factor compared to the 400 GeV proton beam, slip backwards. In order to minimise this effect we set the initial energy of the electron bunch to 30 MeV, a little higher than AWAKE parameters. Typical slip for the beams through 10 m of plasma is illustrated in Fig. 3.

Staying in phase with the drive beam is essential to optimise energy transfer. Establishing an optimal injection point of the electron bunch was achieved by using bunches with length in the order of one λ_p , and tracking a selection of the electrons with optimal energy gain back to $z = 0$.

BEAM LOADING AND ENERGY SPREAD

In a plasma wakefield accelerator, the witness bunch should be accelerated at high efficiency while preserving a low energy spread. Beam loading in the linear regime can be calculated by the linear addition of fields. Only very narrow electron bunches, with $\sigma_r \ll c/\omega_p$, can maintain low energy spread and emittance [7, 8].

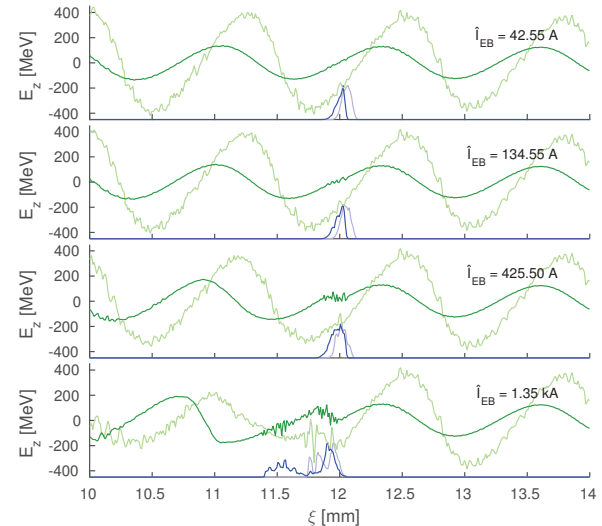


Figure 4: Comparison between the E_z field at 1 m (light green) and 10 m (dark green) of plasma for four different electron bunch currents. The fields are averages over a region $10 - 25 \mu\text{m}$ from the axis. A dimensionless plot of the charge density of the electron bunch is added in blue.

In the non-linear blowout regime, the plasma electrons are blown out by the drive beam, leaving behind a uniform region of plasma ions. The ions pull the electrons back towards the axis, forming a bubble with length on the order of the plasma wavelength [8, 9]. In this regime, the charge and current profile required to optimally load the wake can be estimated analytically. Optimal loading results in a flat E_z field across the bunch with high wake to beam energy transfer efficiency. There is a trade-off between the number of particles that can be accelerated and the accelerating gradient, as discussed in detail by Tzoufras et. al [10].

The beam-plasma interaction studied in this paper has similarities with the above blowout regime, but the train of micro bunches produces a more complex wakefield [4]. We have studied the beam loading through simulations. Based on beam loading in the blowout regime, we use as starting point for the studies a witness bunch with the same peak current as the initial peak current of one proton micro bunch, 135 A. We then performed a scan with logarithmic steps of current from 13.46 A to 13.46 kA. A selection of these are shown in Fig. 4, significant loading of the E_z field does occur when the witness bunch has significantly higher current than the proton beam. An approximate flattening of the field is observed when the witness bunch current is about 3 times higher than the initial micro bunch current, as shown in Fig. 4c. For higher witness bunch currents, we observe that the field from the witness bunch itself starts to dominate the wake it experiences, as expected. The trailing part of the electron bunch is therefore decelerated, as shown for example in Fig. 4d.

We notice that constant loading as the drive and witness bunch propagate in the plasma is not possible, as protons keep being ejected radially throughout the plasma, eating up the micro bunches from the front. This leads to the energy gain levelling off after approximately 4 m of plasma, turning into energy loss as the dephasing between the electron bunch and the E_z fields becomes too large. The phase difference of E_z at 1 m and 10 m is shown in Fig. 4. The mean energy gain (816.2 MeV) and relative energy spread (12%) of the electron bunch, as it travels through the plasma, is visible in blue in Fig. 5, showing a case with peak electron current of 425.5 A. The peak current of a micro bunch after 10 m of plasma, within one skin depth of the axis, is only 45 A.

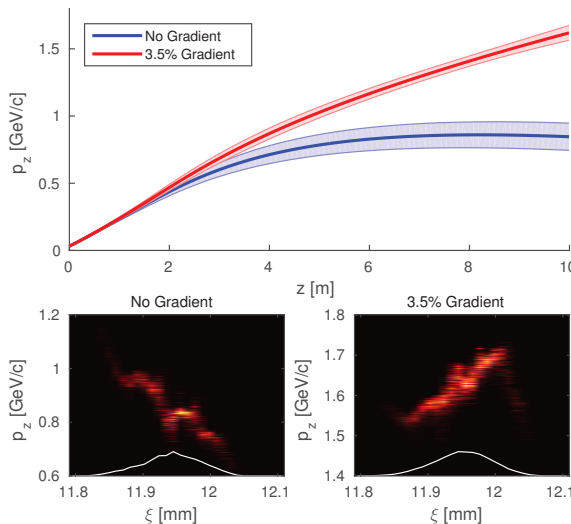


Figure 5: **Top:** Energy gain through 10 m of plasma for a short electron witness bunch with $\sigma_z = 40 \mu\text{m}$ and $\hat{I} = 425.5 \text{ A}$, for the case of no plasma gradient and 3.5% plasma gradient. **Bottom:** $\xi - p_z$ phase plot for both simulations at the end of the plasma.

3: Alternative Particle Sources and Acceleration Techniques

A22 - Plasma Wakefield Acceleration

PLASMA GRADIENT

Due to the backwards drift of the E_z field, the electron bunch falls out of optimal phase after a few metres of plasma. It is possible to stabilise the accelerating bucket by gradually increasing the plasma density. We performed a scan of plasma gradients ranging from 0% to 10% along 10 m of plasma, with a square bunch of length λ_p . We found that a gradient of $0.2 - 0.3 \times 10^{14} \text{ cm}^{-3}$ (3 – 4%) per metre plasma for our initial density of $7 \times 10^{14} \text{ cm}^{-3}$, produced the highest energy gain for the electrons with optimal phase. By tracking some of these electrons back to their injection point, we could move the centre of the short bunch and do a new simulation comparing no gradient to a 3.5% gradient. The best result was for a gradient with a density at 10 m of $7.245 \times 10^{14} \text{ cm}^{-3}$ (3.5%), see Fig. 5 and Table 1.

Table 1: Electron Bunch Energy After 10 m of Plasma

Energy	No Gradient	3.5% Gradient
Mean	846.20 MeV	1618.77 MeV
RMS	101.23 MeV	54.93 MeV
RMS/Mean	11.96 %	3.39 %

CONCLUSION

We have studied beam loading of a SMI proton wake. A scan of electron witness bunch charges over three orders of magnitude revealed that a witness bunch peak current of about a factor 3 higher than the initial peak current of one proton micro bunch was optimal for flattening the wakefield. It is important to note that protons keep getting ejected radially, resulting in a loss of proton charge close to the axis, as the beam travels through the plasma. This decreases the current of a micro bunch by a factor of ~ 3 in the no gradient case.

The electron bunch does not stay in optimal phase for very long as the E_z field starts to drift significantly after 2 – 4 m of plasma. In most simulations the bunch ends up around the zero point of the E_z field, and the energy gradient flattens, and in some cases turns negative. For our optimal case of phase and charge, this effect could to a large degree be counteracted by a 3.5% gradient of the plasma, which forces a positive phase shift of the E_z field, keeping the electron bunch synchronous with the accelerating phase of the wake.

ACKNOWLEDGEMENT

The authors would like to acknowledge the OSIRIS Consortium, consisting of UCLA and IST (Lisbon, Portugal) for the use of OSIRIS, for providing access to the OSIRIS framework.

REFERENCES

- [1] AWAKE Collaboration et al., *Plasma Phys. Control. Fusion* **56**, 084013 (2014).

ISBN 978-3-95450-168-7

2553

- [2] E. Gschwendtner et al., in Proceedings of IPAC2014 (2014), pp. 582–585.
- [3] N. Kumar et al., Phys. Rev. Lett. **104**, 255003 (2010).
- [4] A. Caldwell et al., Phys. Plasmas **18**, 103101 (2011).
- [5] R. A. Fonseca et al., in *Computational science — ICCS 2002*, edited by P. M. A. Sloot et al., Lecture Notes in Computer Science 2331 (Springer Berlin Heidelberg, 2002), pp. 342–351.
- [6] J. Vieira et al., Phys. Plasmas **19**, 063105 (2012).
- [7] T. Katsouleas et al., Part. Acc. **22**, 81–99 (1987).
- [8] M. Tzoufras et al., Phys. Rev. Lett. **101**, 145002 (2008).
- [9] W. Lu et al., Phys. Plasmas **13**, 056709 (2006).
- [10] M. Tzoufras et al., Phys. Plasmas **16**, 056705 (2009).

Publication II

Loading of Wakefields in a Plasma Accelerator Section Driven by a Self-Modulated Proton Beam

Abstract: Using parameters from the AWAKE project and particle-in-cell simulations we investigate beam loading of a plasma wake driven by a self-modulated proton beam. Addressing the case of injection of an electron witness bunch after the drive beam has already experienced self-modulation in a previous plasma, we optimise witness bunch parameters of size, charge and injection phase to maximise energy gain and minimise relative energy spread and emittance of the accelerated bunch.

Authors: Veronica K. Berglyd Olsen, Erik Adli (University of Oslo, Oslo, Norway), Patric Muggli (Max Planck Institute for Physics, Munich, Germany and CERN, Geneva, Switzerland), Jorge M. Vieira (Instituto Superior Technico, Lisbon, Portugal)

Publication: Proceedings of NAPAC 2016, Chicago, Illinois, USA [12]

Date: 9th to 14th of October, 2016

LOADING OF WAKEFIELDS IN A PLASMA ACCELERATOR SECTION DRIVEN BY A SELF-MODULATED PROTON BEAM

V. K. Berglyd Olsen*, E. Adli (University of Oslo, Oslo, Norway)

P. Muggli (Max Planck Institute for Physics, Munich, Germany and CERN, Geneva, Switzerland)

J. M. Vieira (Instituto Superior Technico, Lisbon, Portugal)

Abstract

Using parameters from the AWAKE project and particle-in-cell simulations we investigate beam loading of a plasma wake driven by a self-modulated proton beam. Addressing the case of injection of an electron witness bunch after the drive beam has already experienced self-modulation in a previous plasma, we optimise witness bunch parameters of size, charge and injection phase to maximise energy gain and minimise relative energy spread and emittance of the accelerated bunch.

INTRODUCTION

The AWAKE experiment at CERN proposes to use a proton beam to drive a plasma wakefield accelerator with a gradient on the order of 1 GeV/m to accelerate an electron witness beam [1, 2].

In this paper we present two simulation configurations with a modified proton drive beam based on the baseline parameters for the AWAKE experiment. The drive beam is delivered from the SPS accelerator at CERN at an energy of 400 GeV/c , a bunch length $\sigma_z = 12 \text{ cm}$, and $\sigma_{x,y} = 200 \mu\text{m}$. [3].

The baseline plasma electron density n_{pe} for AWAKE is $7 \times 10^{14} \text{ cm}^{-3}$. The corresponding plasma wavelength $\lambda_{pe} = 2\pi c/\omega_{pe} = 1.26 \text{ mm}$, where $c/\omega_{pe} = 200 \mu\text{m}$ is the plasma skin depth, and ω_{pe} is the plasma frequency given as $[n_{pe} e^2/m_e \epsilon_0]^{1/2}$.

In order to generate a suitable wakefield, the drive beam must be shorter than λ_{pe} . This is not achievable for the SPS proton beam. In order to use such a beam to drive a wakefield we exploit the self-modulation instability (SMI) that can occur when the beam travels through a plasma and $\sigma_z \gg \lambda_{pe}$. The SMI modulates the beam at a period of $\approx \lambda_{pe}$ [4], allowing us to inject the witness beam in an optimal bucket between two such proton micro bunches.

BEAM LOADING

A particle beam at high energy travelling through a plasma will excite a plasma wave in its wake, and the plasma can sustain a very high accelerating gradient [5]. It is possible to accelerate a secondary beam by extracting energy from this wakefield, thus transferring energy from a drive beam to a trailing witness beam. Such an accelerator design was first proposed by Chen in 1985 [6]. However, there are some challenges in this transfer of energy from drive to witness beam.

* v.k.olsen@fys.uio.no

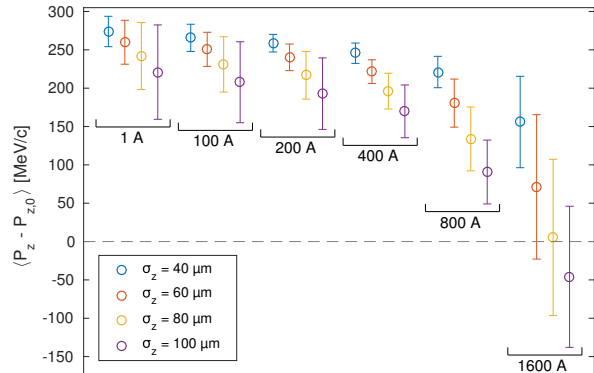


Figure 1: Energy gain and spread for a series of witness beams after $\approx 1.1 \text{ m}$ of plasma. The initial momentum of the witness beam is 217.8 MeV/c . Mean momentum and RMS spread is calculated for all macro particles in the PIC simulation.

One such challenge stems from the witness beam generating its own field, modifying the E_z -field behind it such that the particles in the tail will be accelerated less than those in the front. This causes an increase in energy spread in the beam [7]. This effect can in theory be corrected for by shaping the witness beam. An optimally shaped and positioned beam, such as a triangular beam, can flatten the wakefield such that change in energy spread is effectively zero [8]. However, this requires beam shapes that are difficult to produce experimentally.

BEAM LOADING OF SMI WAKEFIELDS

For AWAKE, most of the SMI evolves during the first stage of $z < 4 \text{ m}$ [2]. This evolution results in a phase change of the wakefields that causes the optimal point for acceleration to drift backwards relative to the witness beam [9, 10].

In our current study we have restricted ourselves to Gaussian witness beams, and seek to demonstrate through simulations how small energy spread can still be achieved by optimally loading the field. The first set of simulations presented uses a subset of 26 micro bunches resulting from the self-modulation that occurs in the previous plasma stage. The pre-modulated beam does undergo further evolution as the envelope function does not fully match the SMI beam, but we only look at the first $\leq 3 \text{ m}$ of this stage, before the phase change starts to dominate [11]. All simulations have been done using OSIRIS 3.0 [12].

A second set of proposed simulations for the second plasma stage will use a single drive beam scaled to produce an accelerating field of 500 MV/m, but with its transverse evolution inhibited in order to study the loading of the field produced by the witness beam alone. The drive beam is short, $\sigma_z = 40 \mu\text{m} \ll \lambda_{pe}$, which is well below the SMI limit.

MULTI DRIVE BUNCH SIMULATIONS

In the multiple drive bunch simulations we assume self-modulation has occurred in a previous stage, and approximate the resulting proton beam in the second stage where acceleration of the witness beam occurs. In this first series of studies we have used a short series of 26 proton bunches with a clipped cosine envelope. This setup is about 10 times shorter than full scale AWAKE simulations, allowing us to run more detailed parameter scans. The setup is described in more detail in our IPAC'15 proceedings, where we looked at beam loading as well as the evolution of the proton beam in a 10 m plasma section [11].

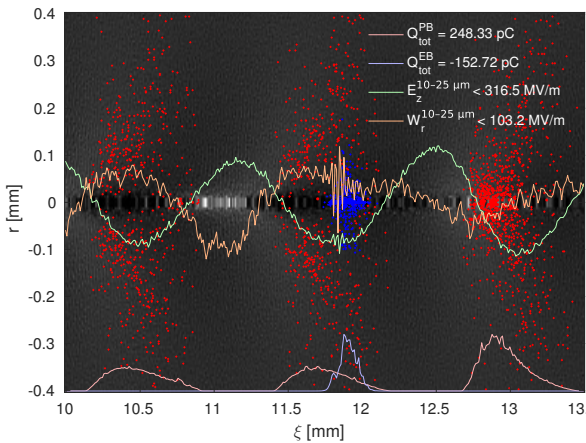


Figure 2: Loading of the field after ≈ 1.1 m of plasma for a 400 A/60 μm electron beam. A sample of electrons (blue) and protons (red) are plotted with their respective projection at the bottom. The total charge within the region of the plot is given as the first two lines of the legend. The longitudinal e-field E_z is shown in green. The transverse wakefield $W_r = E_r - v_z B_\theta$ is shown in orange, where $v_z = c$ is the moving frame of the simulation. The fields are averages over 15 μm near the axis.

The quality and energy of the accelerated witness beam depends on both its position in relation to the field as well as how uniform the field is in the region where the beam is located. We have matched the initial γ of both witness and drive beam in order to avoid initial slipping of the witness beam with relation to the wakefield. The accelerating phase of the field is in the order of $\lambda_{pe}/4 \approx 300 \mu\text{m}$ in length, which puts a constraint on the longitudinal size of the witness beam. The transverse size $\sigma_r = 100 \mu\text{m}$, however we observe in simulations that the beam shrinks by a factor of 4 – 6 as it enters the plasma section. This again results in a sharp

increase in charge density. A scan of different beam sizes and initial beam current and their corresponding energy gain and spread is shown in Fig. 1.

The best result in terms of total energy spread is for the 40 μm beam of an initial current of 200 A, and for the 60 μm beam of an initial current of 400 A. The former beam carries 67 pC and the latter beam 200 pC. As we want to load the field as close to its maximum as possible, this comes at a cost as the tail of the beam will extend beyond the optimal point into the defocusing region of the wakefields. Fig. 2 shows a snapshot of the 60 $\mu\text{m}/400$ A simulation from Fig. 1. The longitudinal field is nearly flat as a result of the loading.

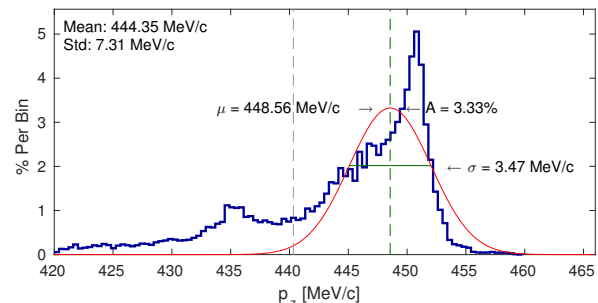


Figure 3: Electron beam momentum spread after ≈ 1.1 m of plasma for the 400 A/60 μm beam. 75 % of the beam charge is accelerated to more than 440 MeV/c, the vertical grey line. The fit is applied to the data above this line, $R^2 = 0.755$.

A closer look at the energy spread in Fig. 3 reveals that ≈ 75 % of the beam is accelerated in this region, with a long tail in energy. This case is not only optimal in terms of beam loading, but also in energy spread of the bulk of the beam of 150 pC. For that part of the beam in front of the grey line we get a relative energy spread $\sigma_{P_z}/[P_z - P_{z,0}] = 1.5$ %. The tail of the beam in terms of energy is lagging behind as it is experiencing defocusing and being pushed outwards and eventually lost from the plasma channel. This loss of beam in the tail can be counteracted by shaping the beam, and making the backwards half $\sigma_z = 20 \mu\text{m}$ and keeping the forward half at $\sigma_z = 60 \mu\text{m}$. In simulations this has reduced this loss to 4 – 5 %. However, such shaping of the beam is technically difficult.

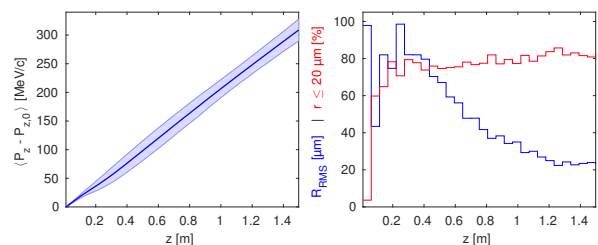


Figure 4: The 400 A/60 μm electron beam as it travels through plasma. The left plot shows the mean energy of the beam with the RMS energy spread as a shaded bar. The right plot shows the RMS radius in blue, and the percentage of macro particles the are within 20 μm of the axis in red.

The relative energy spread of 1.5 % is still undesired. The witness beam in these simulations is initiated with no energy spread in the longitudinal direction. Fig. 4 shows that for our best case the energy spread we see mainly develops in the first 20 cm of plasma. As the right plot illustrates, the transverse RMS size of the beam shrinks by a factor of 5 over the first metres of plasma, but already after a few centimetres about 80 % of the charge is found near the axis. It is this more compact beam that optimally loads the field, and for the first 20 cm the field is under-loaded, probably causing the increase in energy spread. This, however, needs to be studied further.

SINGLE DRIVE BUNCH SIMULATIONS

In order to study the loading of the accelerating e-field in more detail, a second set of simulations have been set up where we have a single proton drive bunch driving a wakefield on the order of 500 MV/m, which is the magnitude of the field we expect to see in the second plasma stage of AWAKE Run 2, based on simulations [13, 14].

This series of simulations is set up in such a way that the accelerating field is as static as possible in order to eliminate other factors than the beam loading by the witness bunch. To achieve this, the proton bunch is prevented from evolving transversely by setting the proton mass to a much higher value than its real value. The gamma of the drive and witness bunches are again matched to prevent dephasing.

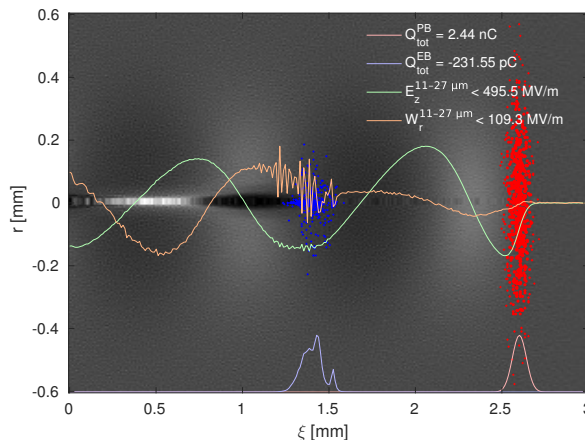


Figure 5: Loading of the field after ≈ 28 cm of plasma for a 500 A/60 μm electron beam. As in Fig. 2 a sample of electrons (blue) and protons (red) are plotted with their respective projections, and the E_z and W_r wakefields are shown.

This provides a much cleaner environment to study the effects of beam loading from the electron beam alone without any evolution caused by the proton beam. Fig. 5 shows an example of this setup. It reproduces the transverse wakefields we saw in our 26 bunch simulations. We also see a shrinking of the witness beam in the first few centimetres, which, together with emittance evolution, is the focus of this next stage of on-going simulation studies.

3: Advanced Acceleration Techniques and Alternative Particle Sources

A22 - Plasma Wakefield Acceleration

CONCLUSION AND CONTINUATION

There are a number of challenges with accelerating an electron beam by a self-modulated proton beam in plasma. Not only does the continued evolution of the proton beam affect the wakefield and thus the acceleration of the witness beam, but the evolution of the witness beam itself affects the wakefields, causing among other things, energy spread. However, by tuning the charge density of the beam, this loading of the field can be used to prevent continuing growth in energy spread provided the phase of the wakefield does not evolve too much.

This is an on-going study, and we are currently looking into the cause of the growth of energy spread. It is worth noting that we have so far run these simulations with an unmatched witness beam. We do see emittance growth in this same region where energy spread increases, but further studies are needed to properly understand the numerical contribution to both these effects.

ACKNOWLEDGEMENTS

The authors would like to acknowledge the OSIRIS Consortium, consisting of UCLA and IST (Lisbon, Portugal), for providing access to the OSIRIS framework.

The numerical simulations have been possible through access to the Abel supercomputer maintained by UNINETT Sigma2 AS, and financed by the Research Council of Norway, the University of Bergen, the University of Oslo, the University of Tromsø and the Norwegian University of Science and Technology. Project code: nn9303k.

REFERENCES

- [1] A. Collaboration, *et al.*, *Plasma Phys. Control. Fusion* 56, 084013 (2014).
- [2] A. Caldwell, *et al.*, *Nucl. Instr. Meth. Phys. Res. A* 829, 3–16 (2016).
- [3] E. Gschwendtner, *et al.*, *Nucl. Instr. Meth. Phys. Res. A* 829, 76–82 (2016).
- [4] N. Kumar, *et al.*, *Phys. Rev. Lett.* 104, 255003 (2010).
- [5] E. Esarey, *et al.*, *IEEE Transactions on Plasma Science* 24, 252–288 (1996).
- [6] P. Chen, *et al.*, *Phys. Rev. Lett.* 54, 693–696 (1985).
- [7] S. Van der Meer, tech. rep. CERN/PS/85-65 (AA), CLIC Note No. 3 (1985).
- [8] T. Katsouleas, *et al.*, *Part. Acc.* 22, 81–99 (1987).
- [9] A. Pukhov, *et al.*, *Phys. Rev. Lett.* 107, 145003 (2011).
- [10] C. B. Schroeder, *et al.*, *Phys. Rev. Lett.* 107, 145002 (2011).
- [11] V. K. B. Olsen, *et al.*, in *Proceedings of IPAC2015* (2015), pp. 2551–2554.
- [12] R. A. Fonseca, *et al.*, in *Computational Science — ICCS 2002*, 2331 (Springer Berlin Heidelberg, 2002), pp. 342–351.
- [13] A. Collaboration, *et al.*, tech. rep. CERN-SPSC-2016-033 (2016).
- [14] E. Adli, *et al.*, in *Proceedings of IPAC2016* (2016), pp. 2557–2560.

Publication III

Data Acquisition and Controls Integration of the AWAKE Experiment at CERN

Abstract: The AWAKE experiment has been successfully installed in the CNGS facility at CERN, and is currently in its first stage of operation. The experiment seeks to demonstrate self-modulation of an SPS proton beam in a rubidium plasma, driving a wakefield of several gigavolt per meter. We describe the data acquisition and control system of the AWAKE experiment, its integration into the CERN control system and new control developments specifically required for AWAKE.

Authors: Veronica K. Berglyd Olsen (University of Oslo, Oslo), Spencer J. Gessner, Jozef J. Batkiewicz, Stephane Deghaye, Edda Gschwendtner (CERN, Geneva, Switzerland), Patric Muggli (Max Planck Institute for Physics, Munich, Germany and CERN, Geneva, Switzerland)

Publication: Proceedings of IPAC 2017, Copenhagen, Denmark [13]

Date: 14th to 19th of May, 2017

DATA ACQUISITION AND CONTROLS INTEGRATION OF THE AWAKE EXPERIMENT AT CERN

Veronica K. Berglyd Olsen*, University of Oslo, Oslo, Norway
 Jozef J. Batkiewicz, Stephane Deghaye, Spencer J. Gessner, Edda Gschwendtner,
 CERN, Geneva, Switzerland
 Patric Muggli, Max Planck Institute for Physics, Munich, Germany and
 CERN, Geneva, Switzerland

Abstract

The AWAKE experiment has been successfully installed in the CNGS facility at CERN, and is currently in its first stage of operation. The experiment seeks to demonstrate self-modulation of an SPS proton beam in a rubidium plasma, driving a wakefield of several gigavolt per meter. We describe the data acquisition and control system of the AWAKE experiment, its integration into the CERN control system, and new control developments specifically required for AWAKE.

device settings and acquired data, as well as subscription to any further data updates [3].

INTRODUCTION

AWAKE is an Advanced Wakefield Experiment designed to demonstrate proton driven plasma wakefield acceleration utilising a 400 GeV proton drive beam from the Super Proton Synchrotron at CERN [1]. The first phase of the experiment has been successfully installed in the former CNGS facility, and was commissioned in October and November 2016.

The first phase of AWAKE is intended to demonstrate the self-modulation instability in the proton drive beam [2], and we had a first short 48 hour run with rubidium plasma and protons in December 2016. Further three weeks of beam time are scheduled at the end of May and in August 2017. The installation of the electron beam phase is scheduled to be completed in September 2017, with first physics expected in November.

CERN CONTROL SYSTEM

Located at CERN, AWAKE is taking advantage of the extensive support infrastructure that already exists for experiments. This also includes integration into the CERN control system.

The Large Hadron Collider is controlled through the Front End Software Architecture (FESA), developed at CERN. This software framework has been extended and generalised in FESA3 to be usable by other experiments as well. FESA device classes are developed based on standardised and modular code tailored for each specific device. These classes are split into a real time and a server process. The real time process is intended to access the hardware directly, and in addition provides access to internal and external timing as well as information from other device classes. The server process provides an interface for get and set operations for

Figure 1: The CERN Control System is structured in three main layers. The Front End Layer consists of VME crates, PCs and PLCs dealing with high performance data acquisition and real time processing. These communicate with application, database and file servers as well as central timing on the Business Layer via the Controls Middleware. Graphical user interfaces and database access are found on the Presentation Layer, and interact with the Business Layer via Java APIs [4].

FESA classes run on Front End Computers (FEC), which run on the Linux operating system. The data from these classes are fed to both data logging systems and control room displays and interfaces as outlined in Fig. 1.

DATA ACQUISITION FOR WINDOWS BASED INSTRUMENTS

The AWAKE experiment has largely been integrated into this infrastructure through direct hardware access between the instruments and the FESA framework. However, some of the instruments depend on proprietary software that is not supported by the standard Front End Computer platform running on Scientific Linux. In order to get around this, and to avoid writing new software, data from three of the instruments currently have to be written to files on shared folders on Windows computers. These files are then imported by designated FESA file reader classes running on CERN supported FECs.

Three instruments currently require software or drivers only available for the Windows operating system:

* v.k.b.olsen@cern.ch

AWAKE uses Mach-Zehnder type interferometers to measure and calculate the vapour density at either end of the 10 m rubidium plasma cell. The acquired interferogram is stored as a file from the instruments software, and a fitting algorithm is applied to calculate the density to within at least $\pm 0.5\%$ relative accuracy [5]. As the fitting is too computationally heavy to run in real time, the fitting is not currently done by the file reader, but will be performed by a separate FESA class running on a dedicated computer.

The rubidium plasma is ionised by a 780 nm, 4.5 TW peak power laser with a pulse length of 100–120 fs [6]. The pulse length is measured by a single shot optical autocorrelator [7]. The autocorrelator itself is a commercial product, and we extract the data directly from its camera through its Windows drivers. On the local computer we compute the projection and fit it with a sech^2 function using Levenberg-Marquardt. We then write the projection, fit, pulse width and the full image to a binary file.

In addition, we have a 4-channel Tektronix oscilloscope with 23 GHz analogue bandwidth and a 50 GSa sampling rate per channel. The oscilloscope is used to measure real time signals from various Schottky diodes installed in a proton beam diagnostic setup downstream of the plasma cell. They measure Coherent Transition Radiation (CTR) emitted in the microwave band. We use proprietary Windows software to automatically save all channel data files at each event trigger.

delay between the time the file is written and when the data is available to the data logging layer. The class polls a dedicated watch folder and attempts to import all files present in reverse chronological order. This is to ensure all data is imported in case of for instance a network interruption. Valid files are then parsed, the data forwarded, and the file itself moved to an archive folder. The original file name of the imported file, as well as its creation time, is stored with the imported data. In the event of an invalid file, a warning is raised and the file is moved to a dropped files folder for later manual verification.

PXI DIGITAL CAMERA SYSTEM

AWAKE uses the analogue camera system provided by the CERN BI group to monitor the proton beam at BTV stations along the beam line. The analogue camera system is radiation hard and requires minimal mechanical upkeep. However, the system is asynchronous to beam extractions. It acquires frames at a fixed rate of 50 FPS and records the frame corresponding to beam extraction. This method of acquisition is not ideal for AWAKE, because AWAKE uses scintillating Chromox screens to image the beam. The scintillation has a long decay time of 140 ms, which is longer than the frame exposure time of 20 ms. This means that under identical experimental conditions, the recorded beam intensity on the screen will vary, simply because the analogue frame is not synced with the beam arrival time.

In addition to this issue, the analogue cameras cannot acquire data at 10 Hz, which is the repetition rate of the laser. For purposes of feedback and stability, it is critical to monitor the laser at this frequency. A digital camera system was implemented to monitor the laser. The camera server is a PXI crate made by National Instruments, and it comprises a trigger and timing system as well as GigE framegrabbers. The digital cameras are made by Basler Ace, and the system supports both CCD and CMOS sensors in a variety of sizes. The image data and camera power are both delivered by a GigE connection using the Power-over-Ethernet (PoE) standard.

The digital camera system was implemented at the laser merging point of the beamline and survived the radiation received during operations in 2016. Because of this success, the digital cameras are being implemented along the beamline to measure both the particle and laser beams. The cameras will be monitored for radiation exposure at areas where high doses are expected in order to understand the total integrated dose (TID) and the single event upset rate (SEU).

EVENT BUILDER

Devices at AWAKE can be read synchronously with SPS beam extractions or asynchronously between extractions. The synchronous/asynchronous distinction depends on the device. For instance, BPMs are read out only when the proton beam is present, but the temperature probes for the Rubidium cell are read out continuously in one second inter-

vals. All of the data from the AWAKE and SPS diagnostics are recorded by the logging system and it is possible to reconstruct the experiment after the fact. It is also desirable to have fast event reconstruction. In order to facilitate this process, the Event Builder was developed to take a “snapshot” of the experiment at the time of the SPS extraction. The Event Builder is subscribed to the key experimental diagnostics, and records their values at the time of extraction, thus providing an instantly correlated dataset comprising both the synchronous and asynchronous variables.

The Event Builder is a JAVA client that is able to subscribe to any variable exposed by the CMW. The Event Builder includes a time-out feature that waits for devices to return data following an extraction. Once the time-out ends, the Event Builder collects the data from all devices and writes them to an HDF5 file, which can be analysed instantly. This data is also copied to the CERN EOS system once per day.

SUMMARY

The integration of the AWAKE experiment into the CERN control system posed a number of challenges. CERN Front End Computers run on Scientific Linux, a platform not supported by all of our instruments. The straight forward solution was to let the Windows based instruments write data dump files on their respective computers, and then use the standard CERN Front End Software Architecture framework to develop file reader classes that can import these via shared network folders.

Due to the relatively large time interval between events, roughly 30 s, the data can be gathered based on time stamps

and collected per event in HDF5 files by an Event Builder. These event files are available immediately after an event, as well as backed up and stored for later analysis.

AWAKE uses many of CERN’s standard analogue and radiation hard cameras. However, these cameras pose synchronisation issues as they have a fixed frame rate of 50 FPS. At critical points, AWAKE uses digital cameras with a trigger and timing system instead.

ACKNOWLEDGEMENTS

The authors would like to thank the AWAKE team at CERN, as well as the CERN Beams, Engineering and Technical Departments for all their assistance in getting the experiment up and running.

REFERENCES

- [1] E. Gschwendtner, et al., in Proceedings of IPAC 2014 (2014), pp. 582–585.
- [2] A. Caldwell, et al., Nucl. Instr. Meth. Phys. Res. A **829**, 3–16 (2016).
- [3] A. Schwinn, et al., in Proceedings of PCaPAC 2010 (2010), pp. 22–26.
- [4] R. Gorbonosov, AWAKE Collaboration Meeting, Apr. 2013.
- [5] E. Öz, F. Batsch, and P. Muggli, Nucl. Instr. Meth. Phys. Res. A **829**, 321–325 (2016).
- [6] E. Gschwendtner, et al., Nucl. Instr. Meth. Phys. Res. A **829**, 76–82 (2016).
- [7] F. Salin, et al., Appl. Opt., AO **26**, 4528–4531 (1987).
- [8] V. K. Berglyd Olsen, 17th AWAKE Technical Board, Feb. 2016.

Publication IV

Emittance Preservation of an Electron Beam in a Loaded Quasi-Linear Plasma Wakefield

Abstract: We investigate beam loading and emittance preservation for a high-charge electron beam being accelerated in quasi-linear plasma wakefields driven by a short proton beam. The structure of the studied wakefields are similar to those of a long, modulated proton beam, such as the AWAKE proton driver. We show that by properly choosing the electron beam parameters and exploiting two well known effects, beam loading of the wakefield and full blow out of plasma electrons by the accelerated beam, the electron beam can gain large amounts of energy with a narrow final energy spread (%-level) and without significant emittance growth.

Authors: Veronica K. Berglyd Olsen, Erik Adli (University of Oslo, Oslo, Norway), Patric Muggli (Max Planck Institute for Physics, Munich, Germany and CERN, Geneva, Switzerland)

Publication: Physical Review Accelerators and Beams [14]

Date:

Emittance preservation of an electron beam in a loaded quasi-linear plasma wakefield

Veronica K. Berglyd Olsen* and Erik Adli
University of Oslo, Oslo, Norway

Patric Muggli
*Max Planck Institute for Physics, Munich, Germany and
 CERN, Geneva, Switzerland*
(Dated: October 16, 2017)

We investigate beam loading and emittance preservation for a high-charge electron beam being accelerated in quasi-linear plasma wakefields driven by a short proton beam. The structure of the studied wakefields are similar to those of a long, modulated proton beam, such as the AWAKE proton driver. We show that by properly choosing the electron beam parameters and exploiting two well known effects, beam loading of the wakefield and full blow out of plasma electrons by the accelerated beam, the electron beam can gain large amounts of energy with a narrow final energy spread (%-level) and without significant emittance growth.

I. INTRODUCTION

Beam driven plasma wakefield accelerators [1] have the potential to offer compact linear accelerators with high energy gradients, and have been of interest for several decades. With a relativistic charged particle drive beam travelling through a plasma, a strong wakefield is excited that can be loaded by a trailing witness beam. When the witness beam optimally loads the wakefield, an increase in absolute energy spread can be kept small. The concept has been demonstrated experimentally in the past using electron drive beams accelerating electron witness beams [2–5].

A major challenge with plasma wakefield accelerators is, however, to accelerate a beam while keeping both energy spread and emittance growth small. In the well described linear regime, valid when the beam density n_b is much smaller than the plasma density n_0 , a non-linear transverse focusing force causes emittance growth of the witness beam. The beam also sees a transversely and longitudinally varying accelerating field causing a spread in energy after the beam has been accelerated [6]. In the non-linear regime, where $n_b > n_0$, a bubble is formed by the transverse oscillations of the plasma electrons, gathering in a sheath around an evacuated area filled with only ions. The ions, assumed stationary, form a uniform density ion channel creating a focusing force that varies linearly with radius. This focusing force preserves emittance [7].

In this paper we present simulation results showing how emittance preservation of a high charge density witness beam can be ensured when accelerated by a proton drive beam producing quasi-linear wakefields [8]. By quasi-linear wakefields we here mean wakefields with only partial blow out of the plasma electrons in the accelerating structure (bubble). The key idea is to have enough charge in the witness beam to at the same time load

the wakefield to produce low relative energy spread, and completely blow out the electrons left in the accelerating structure after the beam to reach conditions that preserves emittance. The results have importance for the preparation of AWAKE Run 2 [9], and possibly other applications in the quasi-linear regime.

A. AWAKE Run 2

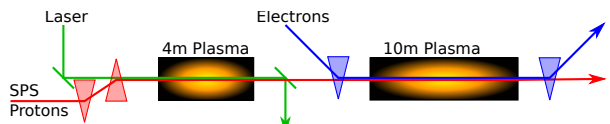


FIG. 1. A simplified illustration of the experimental setup for AWAKE Run 2. The SPS proton beam undergoes self-modulation in the first plasma section. The electron witness beam is injected into the accelerating structure, and undergoes acceleration in the second plasma section [9, 10]

The energy carried by electron drive beams used in previous plasma wakefield experiments have been on the order of 100 J and the propagation length typically no more than 1 m [3, 11]. For high-energy physics application a higher total beam energy is often desired. For instance, the energy of a high-charge electron beam accelerated to 1 TeV with 1×10^{10} electrons, similar to the beam that could be produced by the International Linear Collider, is 1.6 kJ. Using electron beams as drivers, a large number of plasma stages is required to reach an energy of a kJ for the accelerated beam. However, staging plasma accelerators without reducing the effective gradient and spoiling the beam quality is challenging [12, 13].

Proton beams available at CERN carry significantly more energy than available electron beams, 19 kJ for the SPS beam [14], allowing for much longer plasma wakefield accelerator stages. The SPS beam is orders of magnitude longer than the plasma wavelengths needed

* v.k.b.olsen@cern.ch

for such applications, and it does not drive a strong wake [14]. By letting the proton beam undergo self-modulation before injecting the witness beam into the accelerating structure, stronger wakefields are excited. The self-modulation is produced by the transverse fields generated by the beam acting upon itself, causing regions of the beam to rapidly defocus [15]. The modulation frequency is close to that of the plasma electrons, and produces a train of short proton bunches along the beam axis with a surrounding halo of defocused particles. This train of bunches resonantly drives wakefields to large amplitudes.

AWAKE at CERN is a proof of concept proton beam driven plasma wakefield accelerator experiment [16], currently in its first phase of operation. The experiment uses a 400 GeV proton beam delivered by the SPS as its driver, and a single 10 m plasma stage with a nominal plasma density of $7 \times 10^{14} \text{ cm}^{-3}$ [14]. This plasma density corresponds to $\lambda_{pe} = 1.26 \text{ mm}$ and is matched to the transverse size of the proton beam such that $k_{pe}\sigma_{x,y,pb} = 1$ [17], where $k_{pe} = 2\pi/\lambda_{pe}$ is the plasma wave number, $\lambda_{pe} = 2\pi c/\omega_{pe}$, and $\omega_{pe} = (n_0 e^2 / m_e \epsilon_0)^{1/2}$ is the plasma electron angular frequency.

The aim of the first phase of the experiment is to demonstrate self-modulation of the proton beam. The aim of the second phase, in 2018, is to sample the wakefield with a long electron beam ($\simeq \lambda_{pe}$). The study presented here has relevance for Run 2 [9], starting in 2021 after the LHC long shutdown 2, and aims to demonstrate acceleration of a short electron beam ($\ll \lambda_{pe}$) to high energy and with a minimal increase in emittance and absolute energy spread.

The plans for AWAKE Run 2 propose to use two plasma sections, as illustrated in Fig. 1. The first section of about 4 m is the self-modulation stage where the proton beam undergoes self-modulation without the electron beam present. The electron witness beam is then injected into the modulated proton beam before section two where it undergoes acceleration. The self-modulated proton beam does not produce a fully non-linear wakefield, and therefore not all plasma electrons are evacuated from the plasma bubble. The result is that the focusing force does not increase linearly with radius and the accelerated beam emittance is not preserved.

II. METHOD

The focus in this study is on the beam loading of the wakefields driven by the proton beam. Studies of self-modulated proton beams show that the beam evolves as it propagates through a uniform plasma [18], but small variations in the plasma profile the modulation, and thus the wakefields, may be stabilised over long distances [18–20]. To study the witness beam evolution in a stable wake, independent of the dynamics of the self-modulation, we use a single, non-evolving proton bunch as driver. The proton beam parameters are chosen so

that key features of the wake –the plasma electron density in the wake and the longitudinal electric field –are the same as in the wake of a self-modulated proton beam with AWAKE baseline parameters [14]. Both the proton beam and the witness beam have Gaussian longitudinal charge distribution and bi-Gaussian transverse charge distributions.

We have previously studied the beam loading in a proton beam wake using the full particle-in-cell (PIC) code OSIRIS [21] with 2D cylindrical-symmetric simulations. The studies [10, 22] primarily looked at beam loading, energy gain and energy spread, as well as different approaches to creating a stable drive beam structure based on previous self-modulation studies. In order to study the witness beam emittance evolution we use the recently released open-source version of QuickPIC [23, 24]. QuickPIC is a fully relativistic 3D quasi-static PIC code. It does not suffer from the numerical Cherenkov effect that full PIC codes do [25, 26], making it a well suited tool to study emittance preservation. All simulation results in this paper were obtained using QuickPIC open-source [27].

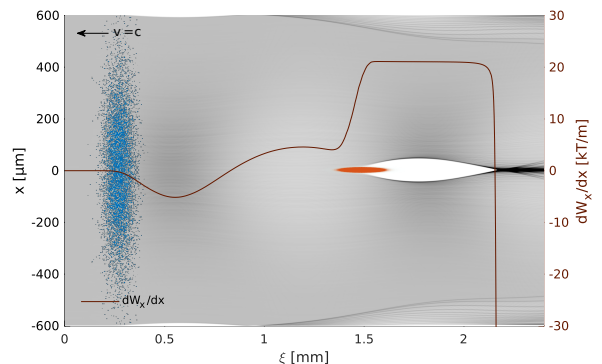


FIG. 2. QuickPIC simulation results showing the initial time step for the single proton drive beam and witness beam setup. Plasma electron density is shown in grey with the drive beam (blue) and the witness beam (red) superimposed. The line plot indicates the transverse wakefield gradient dW_x/dx where $W_x = E_x - v_b B_y$, evaluated along the beam axis. Beams move to the left.

A. Drive Beam Parameters

The modulation process used in AWAKE does not reach the fully non-linear regime and thus does not produce a bubble void of plasma electrons. When the SPS beam, containing 3×10^{11} protons [14], enters the second plasma section (Fig. 1), the peak electric field is expected to be about 500 MV/m. The plasma electron density is only depleted to around 65% of nominal value at the point where we inject the electron beam [28]. The plasma electron density depletion and the peak field are

replicated using a single bunch with 1.46×10^{10} protons (2.34 nC), a length $\sigma_z = 40 \mu\text{m}$ (7 kA), and a transverse size $\sigma_{x,y,pb} = 200 \mu\text{m}$. The beam peak density is $0.83 \cdot n_0$ and results in a quasi-linear wake. To avoid transverse evolution of the proton driver, emulating the stable propagation of the self-modulated beam [18–20], we freeze the transverse evolution of the equivalent proton bunch by increasing the particles mass by six orders of magnitude.

B. Witness Beam Parameters

In order to prevent large amplitude oscillations of the witness beam particles, which may cause additional energy spread as well as emittance growth, we consider a witness beam matched to the plasma density. The matched beam transverse size [29] is:

$$\sigma_{x,y,eb} = \left(\frac{2c^2 \epsilon_N^2 m_e \varepsilon_0}{n_{pe} e^2 \gamma} \right)^{1/4}. \quad (1)$$

We assume an initial normalized emittance of $\epsilon_N = 2 \mu\text{m}$. This emittance is possible to produce with a standard RF-injector, while at the same time yielding a sufficiently narrow beam.

Beam loading by a short witness beam is sensitive to its position relative to the electric field [30] as well as, at low energy, to its de-phasing with respect to the wakefields. To eliminate de-phasing of the witness beam, the initial beam energy is set such that $\gamma_{eb} = \gamma_{pb} = 426.3$, giving an energy of 217 MeV. A lower initial energy is likely to be sufficient for AWAKE Run 2 injection.

Equation (1) yields a transverse size $\sigma_{x,y,eb}$ of 5.25 μm , which is narrow compared to the drive beam $\sigma_{x,y,pb} = 200 \mu\text{m}$. The bunch length was set to $\sigma_z = 60 \mu\text{m}$ based on earlier beam loading studies [22]. The charge is adjusted to 100 pC for optimal beam loading, as discussed in the next section. We refer to the defined drive beam and witness beam parameter set as the *base case*. Figure 2 shows the two beams – the proton beam in blue, the trailing electron beam in red, and the plasma electron density in grey – from a QuickPIC simulation of the initial time step, for the base case parameters.

C. Simulation parameters

The relatively small size of the witness beam puts constraints on the transverse grid cell size and number in the simulations. We need a small size to resolve the narrow electron beam, and a large number of grid cells to resolve the much wider proton beam and its wakefields. We use a transverse grid cell size of 1.17 μm , and of 2.34 μm for the longitudinal grid cells for the simulations presented in section III. The witness beam was simulated with 16.8×10^6 and the drive beam with 2.1×10^6 non-weighted particles, and the plasma electrons with 1024×1024 weighted particles per transverse slice.

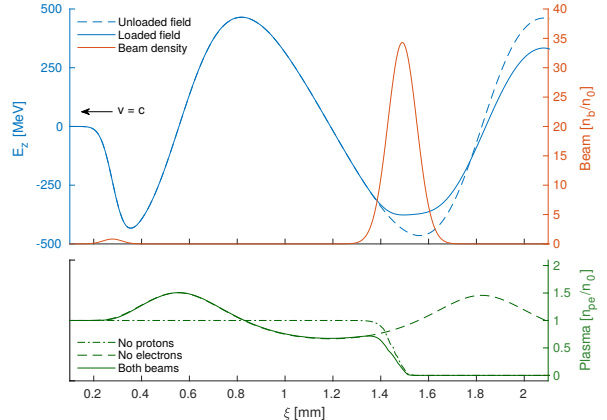


FIG. 3. Top plot: Unloaded longitudinal electric field with no witness beam (dashed blue line) and loaded field (whole blue line) along the beam axis. The beam density along the axis for both beams are shown in red. Bottom plot: Plasma densities along the beam axis for a drive beam with no witness beam (dashed green line), witness beam with no drive beam (dash-dotted green line), and both beams present (continuous green line). The position in the simulation box $\xi = z - tc$, moving towards the left. The plots show the initial time step.

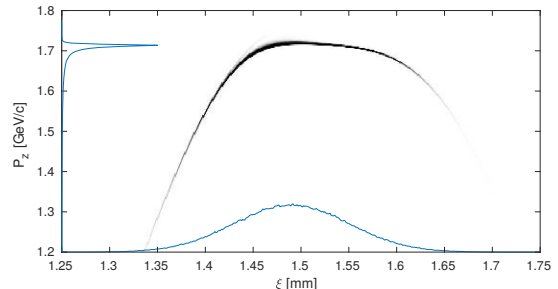


FIG. 4. Longitudinal phase space charge distribution of a 100 pC, 60 μm long witness beam after 4 m of plasma. The mean momentum is 1.67 GeV/c with an RMS energy spread of 87 MeV/c (5.2%) for the full beam.

III. BEAM LOADING

Figure 3 shows the results of QuickPIC simulations of the initial time step for the base case parameters. The E_z -field generated by the proton drive beam is seen as the blue line, shown with and without the electron beam present. With a proton beam density $n_{pb} \simeq n_0$, the wakefields are in the quasi-linear regime [8]. The dashed green line in the lower part of Fig. 3 shows that the on-axis plasma density has a depletion to 67%, close to what we see in full scale reference simulations for AWAKE Run 2 [28].

The witness beam generates its own wakefield that loads the E_z -field generated by the drive beam. With an

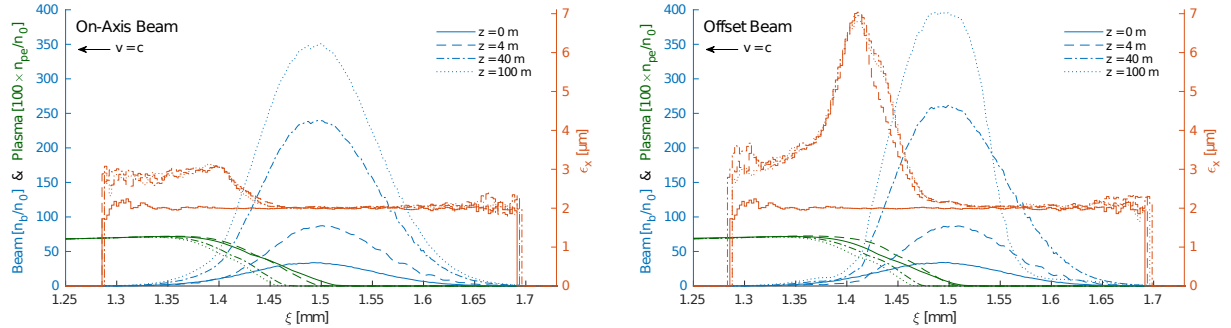


FIG. 5. Beam density in blue along the beam axis for an on-axis beam with respect to the drive beam axis (left), and an offset beam (right) with an offset of one $\sigma_{x,eb} = 5.24 \mu\text{m}$ in the x-plane –at four different positions z in the plasma stage. The red lines show a moving window calculation of transverse normalised emittance. The moving window calculation uses longitudinal slices of $l = 4 \cdot \Delta\xi = 9.38 \mu\text{m}$ with a step of $\Delta\xi$. Only slices with more than 100 macro particles have been included. The plasma density profile is included in green, and scaled up by a factor of 100 to be visible. These simulations were run with an LHC energy drive beam of 7 TeV

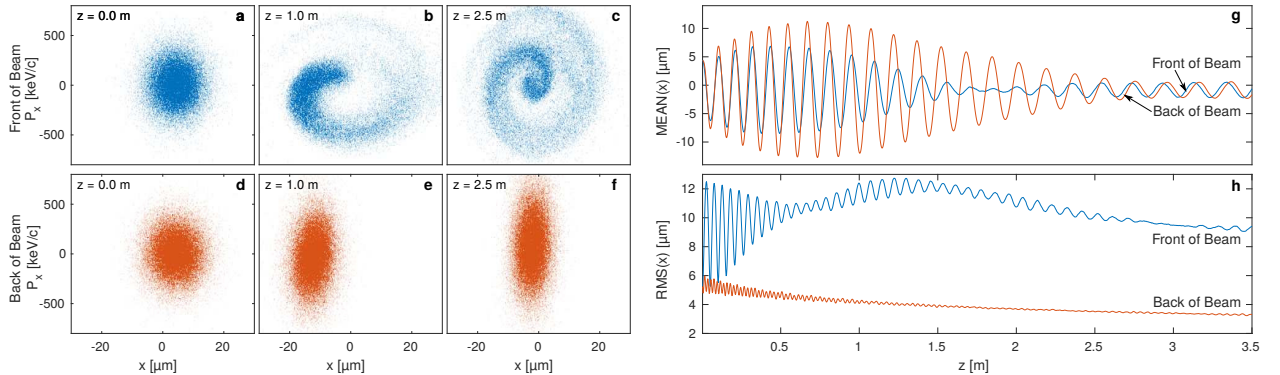


FIG. 6. Plots **a** to **f** show the transverse phase space of the offset electron beam at different plasma positions. Plot **g** shows the macro particle mean position, and plot **h** their RMS spread. Plots **a**, **b** and **c**, as well as the blue lines in plots **g** and **h** represent particles not in the ion column (see Fig. 5), with position $1.40 \mu\text{m} < \xi < 1.42 \mu\text{m}$. Plots **d**, **e** and **f**, and the red lines in plots **g** and **h** represent particles in the ion column with position $1.55 \mu\text{m} < \xi < 1.57 \mu\text{m}$.

ideally shaped electron beam charge profile it is possible to optimally load the field in such a way that the accelerating field is constant along the beam [6, 30]. Gaussian beams, as assumed in these studies, cannot completely flatten the electric field in the tails of the charge distribution, and our base case beam therefore has a tail in energy both at the front and the back of the beam, as illustrated in Fig. 4. The bulk of the beam, however, sees a relatively flat field.

The initial electron beam density is $n_{eb} \approx 35 \cdot n_0$. This means that the witness beam's own wakefield is in the fully non-linear regime, where the space charge force is sufficient to blow out all plasma electrons, resulting in the formation of a pure ion column (see Fig. 3, bottom). This ion column, as is well known [7], provides a linear focusing force on the part of the electron beam within the column, and therefore prevents emittance growth for this part of the beam. This bubble and the focusing force is

shown for our base case in Fig. 2. The focusing field has a gradient of 20 kT/m near the beam axis, corresponding to the matched field gradient.

Figure 5 shows the slice emittance along the beam for the base case, sampled after propagating through 0, 4, 40 and 100 m of plasma. We define emittance of a slice as preserved if the growth is less than 5%, and \tilde{Q} as the sum charge of the slices for which the emittance is preserved. Simulation results show that $\tilde{Q}/Q = 73\%$ of the electron beam longitudinal slices retain their initial emittance after the propagation in the plasma. The total (projected) emittance of these slices combined is also preserved. Emittance growth mainly occurs in the first few metres, and no significant emittance growth is observed after this for propagation lengths up to 100 m. The head of the beam does not benefit from the full ion column focusing, but since the proton beam creates a quasi-linear wake, the emittance of the head of the beam still sta-

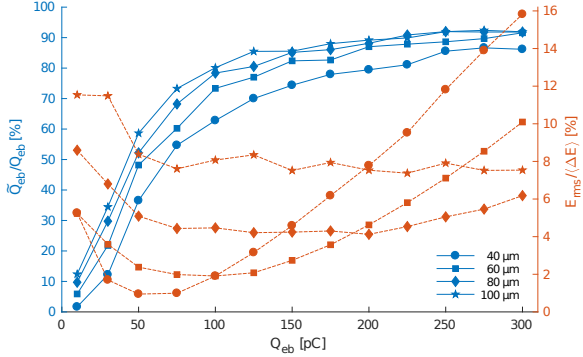


FIG. 7. Ratio of witness beam charge with emittance preserved, \tilde{Q}/Q (blue symbols, lines), and relative energy spread of the accepted charge (red symbols, dashed lines), after 4 m of plasma and with an initial emittance $\epsilon_{N,0} = 2 \mu\text{m}$. These are shown for four different σ_z from $40 \mu\text{m}$ to $100 \mu\text{m}$. The detailed studies presented in beam loading section correspond to the square marked lines at 100 pC .

bilises after some time. For the 100 m simulation, the drive beam energy was increased to 7 TeV (LHC energy) to prevent de-phasing, as de-phasing starts to become a significant effect for the SPS beam of 400 GeV after about 50 m.

So far we have considered a witness beam injected on the axis of the proton beam. We now briefly examine the case of injection of a witness beam with an offset with respect to the proton beam axis. Since the witness beam creates its own plasma bubble, the emittance of the part of the beam inside that bubble is not affected by small transverse offsets of the witness beam with respect to the proton beam axis. This is illustrated in Fig. 5, right, for an electron beam offset of one $\sigma_{x,\text{eb}}$. Emittance preservation for small offsets is an added benefit of this accelerating regime, and may ease transverse injection tolerances. The head of the beam experiences a larger initial emittance growth than for the on-axis case (compare Fig. 5, left, to Fig. 5, right). However, also for the head of the beam the emittance growth ends after the first few metres. Figure 6a-c show the phase space of the head of the electron beam after 0, 1.0 and 2.5 m, while Fig. 6d-f show the phase space of the trailing part of the beam. The centroid oscillations of the head and the trailing part are shown in Fig. 6g. This effect of a transverse offset is greater for larger offsets as the beam oscillates around the axis of the drive beam wakefield.

The transverse beam size within the bubble, where normalised emittance is preserved, follows the evolution given by Eq. 1; that is, evolves to stay matched. The on-axis density of the electron beam, as a result, increases as its gamma factor increases and its transverse size decreases. This effect can be seen in Fig. 6h. This has the potential to cause overloading of the field. However, for the base case no significant overloading is observed.

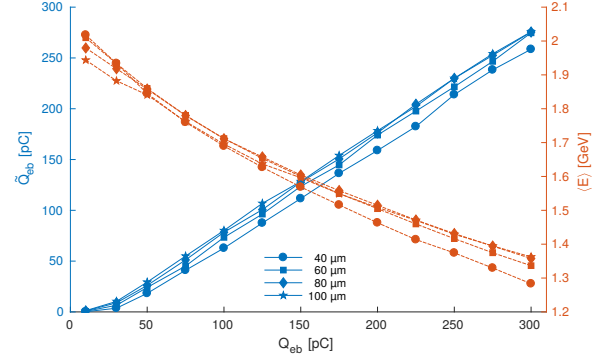


FIG. 8. Witness beam charge with emittance preserved, \tilde{Q} (blue symbols, lines), and final energy (red symbols, dashed lines), after 4 m of plasma and with an initial emittance $\epsilon_{N,0} = 2 \mu\text{m}$.

Parameters can also be chosen in order to minimise this effect by slightly underloading the wakefield at first, and let the high energy beam overload the wakefield at the end.

IV. PARAMETER OPTIMISATION

The beam loading and blow out properties of the electron beam depend on a large number of parameters, including longitudinal profile, transverse profile, as well as relative phasing of the proton and the electron beams. We present a limited parameter study aimed to guide beam parameter choices for AWAKE Run 2. For an electron beam to be externally injected in AWAKE Run 2 (see Fig. 1) it is desired to maximise the energy gain, minimise the energy spread, maximise the charge to be accelerated, and minimise the emittance growth [9]. In addition, the beam length should be such that it is possible to generate and transport the beam using a compact electron injector [9]. We investigate the interdependence of these parameters in simulation by varying the electron beam length, its charge, and initial emittance. The results are quantified in terms of how much of the beam retains its initial emittance. For these parameter scans we used a transverse grid cell size of $2.34 \mu\text{m}$, and let the beams propagate through 4 m of plasma.

Figure 7 shows the dependence of charge and energy spread on witness beam length and incoming charge. An initial beam emittance of $2 \mu\text{m}$ was used. Therefore, we define the fractional charge \tilde{Q} as the charge whose emittance remains smaller than $2.1 \mu\text{m}$. The beam charge ranges from 10 pC to 300 pC, and σ_z ranges from $40 \mu\text{m}$ to $100 \mu\text{m}$. As can be seen from Fig. 7 (red curves),

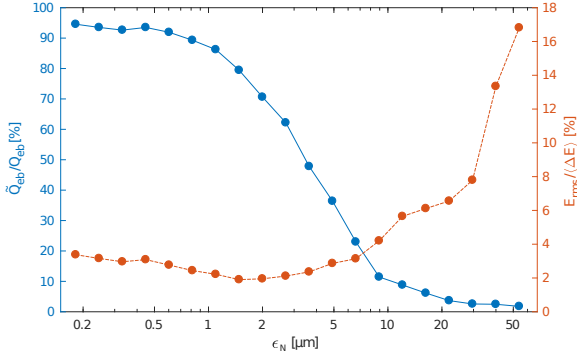


FIG. 9. Ratio of witness beam charge with emittance preserved, \tilde{Q}/Q (blue symbols, line), as a function of beam initial emittance (right), with relative energy spread of the accepted charge (red symbols, dashed line), after 4 m of plasma.

both the $40\text{ }\mu\text{m}$ and the $60\text{ }\mu\text{m}$ beams have a well defined minimum energy spread with an initial beam charge $\approx 50\text{ pC}$ and $\approx 100\text{ pC}$, respectively. Lower beam charges tend to underload the electric field, while higher beam charges tend to overload it. It is also clear that longer beams with respect to the accelerating phase of the field, $\approx \lambda_{pe}/4$, do not optimally load the wake, thus producing a larger spread in energy. The blue curves show the fraction of charge whose initial emittance is preserved (the slice emittance for the base case is shown in Fig. 5). As the witness beam charge increases, the fraction of slices with preserved emittance increases –as expected from an earlier onset of the bubble formation –and also increases in the bubble size [31, 32]. We note here that operation with 100 pC leads to a significantly larger charge (factor ~ 4) with emittance preserved, at the expense of an increase of relative energy spread by a factor of two.

Figure 8 shows the dependence of mean energy gain on beam length and beam charge (red curves). The blue curves show the amount of charge in the longitudinal slices where the emittance has been preserved, as a function of beam length and beam charge. The results are weakly dependent on the electron beam length. As expected, a larger value of \tilde{Q} corresponds to a lesser energy gain. No optimum is observed.

Figure 9 shows how the growth in emittance and energy spread varies with initial electron beam emittance. In these simulations we adjusted the witness beam radius to maintain the matching condition at each emittance. The smaller the initial emittance is, the better the emittance is preserved. There are two effects that lead to emittance growth for high initial emittance beams: the transverse beam size may increase beyond the size of the bubble, and the beam density may be reduced so much that the plasma electrons are no longer fully evacuated from the bubble. Emittance values higher than a few micrometres lead to a significant increase in both emittance and energy spread.

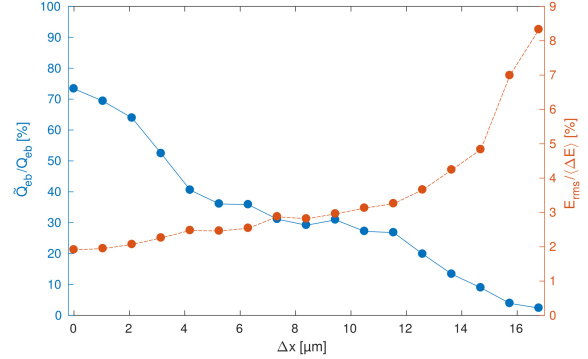


FIG. 10. Ratio of witness beam charge with emittance preserved, \tilde{Q}/Q (blue symbols, line), as a function of beam offset, with relative energy spread of the accepted charge (red symbols, dashed line), after 4 m of plasma.

Our base case showed some robustness to a small offset from the proton beam axis on the order of one $\sigma_{x,eb}$, but with a reduction of the fraction of the beam which retains its initial emittance. Figure 10 shows the correlation between this ratio for a range of offsets up to $16.8\text{ }\mu\text{m}$, corresponding to $3.2 \cdot \sigma_{x,eb}$. The effect on the head of the beam, shown in Figs. 5 and 6, increases with larger offsets causing the part of the beam being defocused to extend backwards to the point where the witness beam wakefields are no longer in the blow-out regime. At around $3 \cdot \sigma_{x,eb}$ emittance is no longer preserved at all.

The optimal working point will depend on the application and must be studied for each case and is, as illustrated in this section, a trade off between beam length, beam charge and emittance preservation, as well as other parameters like the plasma density.

V. CONCLUSION

We have devised a method to accelerate an electron witness beam to high energy with a low relative energy spread while maintaining its incoming emittance in wakefields such that the accelerating structure is not void of plasma electrons. This is the case for the AWAKE experiment in which the wakefields are driven by a train of proton bunches produced by self-modulation of a long proton beam. This method is in principle applicable to all experiments operating in the quasi-linear regime. Low relative energy spread and emittance preservation are achieved by choosing the electron beam parameters to load the wakefields and evacuate the remaining plasma electrons from the accelerating structure.

Parameter studies indicate that for up to a few 100 pC , about 70% of the incoming beam charge is accelerated for beam lengths of $40 - 60\text{ }\mu\text{m}$. Such electron beams may be generated by an injector based on a standard RF photo-emission gun [33].

In order to use manageable computer time for simulations, this study assumes a simplified case with respect to a self-modulated proton beam, where the wake is driven by a single, short proton bunch producing similar wakefields. However, the wakefields driven by a train of bunches evolve with the ramp of a real plasma and when entering the plasma. Therefore, to be fully applicable to an experiment such as AWAKE, the study will have to be redone with more realistic parameters. However, using loading of the wakefields and the pure plasma ion column fields to produce an accelerated beam with low relative energy spread and emittance remains applicable.

VI. ACKNOWLEDGEMENTS

The simulations for this study have been performed using the open source version of QuickPIC released in

early 2017 and owned by UCLA.

These numerical simulations have been made possible through access to the *Abel* computing cluster in Oslo, Norway. Abel is maintained by UNINETT Sigma2 AS and financed by the Research Council of Norway, the University of Bergen, the University of Oslo, the University of Tromsø and the Norwegian University of Science and Technology. Project code: nn9303k. Some of the simulations were also run on the student-maintained computing cluster *Smaug* at the University of Oslo, Department of Physics.

We gratefully acknowledge helpful discussions with Jorge Vieira from IST, Lisbon.

-
- [1] P. Chen, J. M. Dawson, R. W. Huff, and T. Katsouleas, *Physical Review Letters* **54**, 693 (1985).
 - [2] J. B. Rosenzweig, D. B. Cline, B. Cole, H. Figueroa, W. Gai, R. Konecny, J. Norem, P. Schoessow, and J. Simpson, *Physical Review Letters* **61**, 98 (1988).
 - [3] I. Blumenfeld, C. E. Clayton, F.-J. Decker, M. J. Hogan, C. Huang, R. Ischebeck, R. Iverson, C. Joshi, T. Katsouleas, N. Kirby, W. Lu, K. A. Marsh, W. B. Mori, P. Muggli, E. Oz, R. H. Siemann, D. Walz, and M. Zhou, *Nature* **445**, 741 (2007).
 - [4] E. Kallos, T. Katsouleas, W. D. Kimura, K. Kusche, P. Muggli, I. Pavlishin, I. Pogorelsky, D. Stolyarov, and V. Yakimenko, *Physical Review Letters* **100**, 074802 (2008).
 - [5] M. Litos, E. Adli, W. An, C. I. Clarke, C. E. Clayton, S. Corde, J. P. Delahaye, R. J. England, A. S. Fisher, J. Frederico, S. Gessner, S. Z. Green, M. J. Hogan, C. Joshi, W. Lu, K. A. Marsh, W. B. Mori, P. Muggli, N. Vafaei-Najafabadi, D. Walz, G. White, Z. Wu, V. Yakimenko, and G. Yocky, *Nature* **515**, 92 (2014).
 - [6] T. Katsouleas, S. Wilks, P. Chen, J. M. Dawson, and J. J. Su, *Particle Accelerators* **22**, 81 (1987).
 - [7] J. B. Rosenzweig, B. Breizman, T. Katsouleas, and J. J. Su, *Physical Review A* **44**, R6189 (1991).
 - [8] J. B. Rosenzweig, G. Andonian, M. Ferrario, P. Muggli, O. Williams, V. Yakimenko, and K. Xuan, *AIP Conference Proceedings* **1299**, 500 (2010).
 - [9] E. Adli and AWAKE Collaboration, in *Proceedings of IPAC 2016*, International Particle Accelerator Conference (JACoW, Busan, Korea, 2016) pp. 2557–2560.
 - [10] V. K. Berglyd Olsen, E. Adli, P. Muggli, L. D. Amorim, and J. Vieira, in *Proceedings of IPAC 2015* (Richmond, VA, USA, 2015) pp. 2551–2554.
 - [11] A. Caldwell, K. Lotov, A. Pukhov, and F. Simon, *Nature Physics* **5**, 363 (2009).
 - [12] S. Steinke, J. van Tilborg, C. Benedetti, C. G. R. Geddes, C. B. Schroeder, J. Daniels, K. K. Swanson, A. J. Gonsalves, K. Nakamura, N. H. Matlis, B. H. Shaw, E. Esarey, and W. P. Leemans, *Nature* **530**, 190 (2016).
 - [13] C. A. Lindström, E. Adli, J. M. Allen, J. P. Delahaye, M. J. Hogan, C. Joshi, P. Muggli, T. O. Raubenheimer, and V. Yakimenko, *Nuclear Instruments and Methods in Physics Research Section A* **829**, 224 (2016).
 - [14] E. Gschwendtner, E. Adli, L. Amorim, R. Apsimon, R. Assmann, A. M. Bachmann, F. Batsch, J. Bauche, V. K. Berglyd Olsen, M. Bernardini, R. Bingham, B. Biskup, T. Bohl, C. Bracco, P. N. Burrows, G. Burt, B. Buttenschön, A. Butterworth, A. Caldwell, M. Cassella, E. Chevallay, S. Cipiccia, H. Damerau, L. Deacon, P. Dirksen, S. Doeberl, U. Dorda, J. Farmer, V. Fedosseev, E. Feldbaumer, R. Fiorito, R. Fonseca, F. Friebel, A. A. Gorn, O. Grulke, J. Hansen, C. Hessler, W. Hofle, J. Holloway, M. Hüther, D. Jaroszynski, L. Jensen, S. Jolly, A. Joulaei, M. Kasim, F. Keeble, Y. Li, S. Liu, N. Lopes, K. V. Lotov, S. Mandry, R. Martorelli, M. Martyanov, S. Mazzoni, O. Mete, V. A. Minakov, J. Mitchell, J. Moody, P. Muggli, Z. Najmudin, P. Norreys, E. Öz, A. Pardons, K. Pepitone, A. Petrenko, G. Plyushchev, A. Pukhov, K. Rieger, H. Ruhl, F. Salveter, N. Savard, J. Schmidt, A. Seryi, E. Shaposhnikova, Z. M. Sheng, P. Sherwood, L. Silva, L. Soby, A. P. Sosedkin, R. I. Spitsyn, R. Trines, P. V. Tuev, M. Turner, V. Verzilov, J. Vieira, H. Vincke, Y. Wei, C. P. Welsch, M. Wing, G. Xia, and H. Zhang, *Nuclear Instruments and Methods in Physics Research Section A* **829**, 76 (2016).
 - [15] N. Kumar, A. Pukhov, and K. Lotov, *Physical Review Letters* **104**, 255003 (2010).
 - [16] AWAKE Collaboration, R. Assmann, R. Bingham, T. Bohl, C. Bracco, B. Buttenschön, A. Butterworth, A. Caldwell, S. Chattopadhyay, S. Cipiccia, E. Feldbaumer, R. A. Fonseca, B. Goddard, M. Gross, O. Grulke, E. Gschwendtner, J. Holloway, C. Huang, D. Jaroszynski, S. Jolly, P. Kempkes, N. Lopes, K. Lotov, J. Machacek, S. R. Mandry, J. W. McKenzie, M. Meddahi, B. L. Militsyn, N. Moschuering, P. Muggli, Z. Najmudin, T. C. Q. Noakes, P. A. Norreys, E. Öz, A. Pardons, A. Petrenko, A. Pukhov, K. Rieger, O. Reimann, H. Ruhl, E. Shaposhnikova, L. O. Silva, A. Sosedkin, R. Tarkeshian, R. M. G. N. Trines, T. Tückmantel,

- J. Vieira, H. Vincke, M. Wing, and G. Xia, *Plasma Physics and Controlled Fusion* **56**, 084013 (2014).
- [17] W. Lu, C. Huang, M. M. Zhou, W. B. Mori, and T. Katsouleas, *Physics of Plasmas* **12**, 063101 (2005).
- [18] K. V. Lotov, *Physics of Plasmas* **18**, 024501 (2011).
- [19] K. V. Lotov, *Physics of Plasmas* **22**, 103110 (2015).
- [20] A. Caldwell and K. V. Lotov, *Physics of Plasmas* **18**, 103101 (2011).
- [21] R. A. Fonseca, L. O. Silva, F. S. Tsung, V. K. Decyk, W. Lu, C. Ren, W. B. Mori, S. Deng, S. Lee, T. Katsouleas, and J. C. Adam, in *Computational Science — ICCS 2002*, Lecture Notes in Computer Science No. 2331, edited by P. M. A. Sloot, A. G. Hoekstra, C. J. K. Tan, and J. J. Dongarra (Springer Berlin Heidelberg, 2002) pp. 342–351.
- [22] V. K. Berglyd Olsen, E. Adli, P. Muggli, and J. Vieira, in *Proceedings of NAPAC 2016* (Chicago, IL, USA, 2016).
- [23] C. Huang, V. K. Decyk, C. Ren, M. Zhou, W. Lu, W. B. Mori, J. H. Cooley, T. M. Antonsen, and T. Katsouleas, *Journal of Computational Physics* **217**, 658 (2006).
- [24] W. An, V. K. Decyk, W. B. Mori, and T. M. Antonsen, *Journal of Computational Physics* **250**, 165 (2013).
- [25] B. B. Godfrey, *Journal of Computational Physics* **15**, 504 (1974).
- [26] R. Lehe, A. Lifschitz, C. Thaury, V. Malka, and X. Davoine, *Physical Review Special Topics - Accelerators and Beams* **16**, 021301 (2013).
- [27] UCLA Plasma Simulation Group, “QuickPIC-OpenSource,” GitHub repository (2017).
- [28] AWAKE Collaboration and A. Caldwell, *AWAKE Status Report, 2016*, Tech. Rep. CERN-SPSC-2016-033 (CERN, Geneva, 2016).
- [29] E. Esarey, P. Sprangle, J. Krall, and A. Ting, *IEEE Transactions on Plasma Science* **24**, 252 (1996).
- [30] M. Tzoufras, W. Lu, F. S. Tsung, C. Huang, W. B. Mori, T. Katsouleas, J. Vieira, R. A. Fonseca, and L. O. Silva, *Physics of Plasmas* **16**, 056705 (2009).
- [31] W. Lu, C. Huang, M. Zhou, W. B. Mori, and T. Katsouleas, *Physical Review Letters* **96**, 165002 (2006).
- [32] W. Lu, C. Huang, M. Zhou, M. Tzoufras, F. S. Tsung, W. B. Mori, and T. Katsouleas, *Physics of Plasmas (1994-present)* **13**, 056709 (2006).
- [33] S. Doeberl, private correspondence (2017).

Appendices

Appendix A

Particle in Cell (PIC)

Some stuff about PIC codes

A.1 Full PIC

OSIRIS [29, 30]

A.2 Quasi-Static PIC

QuickPIC [4, 37]

A.3 Numerical Cherenkov

The effect [31, 32]

Yee solver [73]

Lehe solver [44]

Appendix B

Data Analysis

The simulation codes used in these studies produce large amounts of data. It has been very useful to develop a tool for effective analysis of bot input and output files. Most of the initial studies were done using OSIRIS (Publication I and II), and the final emittance study was done using QuickPIC (Publication IV).

The analysis code written for these studies are publicly available on GitHub. The toolbox for OSIRIS is named OsirisAnalysis [9], and the corresponding toolbox for QuickPIC is named QuickPICAAnalysis [10]. Both toolboxes are written in MATLAB.

This appendix briefly outlines the structure and basic function of these tools.

B.1 Osiris Analysis Toolbox

The OsirisAnalysis toolbox is a modular and object oriented data analysis toolbox written in MATLAB. It was designed as a three layer tool to wrap a single data set of OSIRIS simulation data:

- **Layer 1** consists of the core data wrapper class OsirisData with its subclass OsirisConfig. The OsirisData class provides an interface for accessing the raw data files, while the OsirisConfig class parses the simulation input file. OsirisData provides a uniform set of calls for extracting the data, and gives through OsirisConfig access to all the simulation parameters and conversion factors for converting Osiris' normalised units into SI units.
- **Layer 2** consists of a set of classes that takes an OsirisData object as input, and returns standardised structs of data that can be scaled and converted to preferred units. They perform often needed tools and methods to parse data and extract more detailed information from the larger raw datasets.
- **Layer 3** consist of a number of useful standardised plots, and a GUI tool to quickly do a preliminary analysis of simulation data.

The idea behind this layering of the analysis tool is to allow the user to choose how many of these they will use. Only using the first layer will give the user access to all the simulation parameters as well as a method to extract data in a standardised manner and return a simple matrix of its content. Adding the second layer gives additional access to automatic unit conversion and other data conversion tools like slicing and lineouts, as well as various properties extracted from

the macro particle arrays. The third layer provides a quick way to browse through the datasets and display density plots, phasespace plots, Twiss parameters, time evolution, etc.

B.1.1 OsirisAnalysis Core Objects

The innermost layer consists of two classes OsirisData and OsirisConfig.

The OsirisData class wraps the simulation data folder and is the core interface through which data is extracted. The class also provides some simple methods for extracting information about the dataset like physical dimensions of the beam and the distribution of the plasma.

The OsirisConfig class is a wrapper for the input file itself, and contains a parser for this file which extracts all the relevant information for both analysis and provides lists of available diagnostics for the graphical user interface (GUI). All conversion factors to SI units are calculated on the fly when the input file is loaded. The OsirisConfig class is not intended to be called by the user, but is found as a child object of the OsirisData data object.

B.1.2 OsirisAnalysis Data Types

The secondary layer of the OsirisAnalysis framework is a set of subclasses under a parent class named OsirisType. The subclasses will give access to specific types of data more or less directly related to the diagnostics types produced by the OSIRIS simulation code.

The classes provided are:

- **Density and Field:** These are classes that produce grid diagnostics data for the particle density data dumps or the field diagnostics data. They support all the different density diagnostics outputs of Osiris, and will in addition calculate the wakefields from the magnetic and electric fields given by $W = F/q = E - v \times B$.
- **Momentum:** The Momentum class consists of a set of methods that will calculate the evolution of the beams energy and momentum over several time dumps.
- **Phase:** The Phase class provides several tools for phase space diagnostics, including calculations of Twiss parameters.
- **UDist:** This class is similar to the Density and Field classes, and provides methods to process velocity and thermal distribution data.
- **Species:** The Species class provides a few additional specialised tools for calculating energy deposition and gain into and from the plasma by the beams, and is also the class where particle tracking data is parsed.

In addition to these data parsing classes, there is also a Variables class that will translate Osiris diagnostics variables into readable forms and into strings usable for plot labels. There is also a MathFunc class that provides a math parser that emulates the one used by OSIRIS to parse mathematical functions from the input files. This class is mainly used to extract geometric information about beam density based on the function provided in the input file without the need to first run the code to provide raw particle data.

B.1.3 OsirisAnalysis Graphical Interface and Plots

The final layer of the OsirisAnalysis framwork is a set of very flexible plotting tools. Most of them have a long list of optional input argument. Most of these optional arguments are available through a graphical interface also written in MATLAB named AnalysisGUI.

B.2 QuickPIC Analysis Framework

The toolbox developed for OSIRIS was also partially rewritten to work with QuickPIC simulations. As QuickPIC uses more or less the same normalised units, the code required little modification to work with these output files. The conversion was also made easier by QuickPIC having a simpler and more consistent set out output files and formats.

Only the core objects and input file wrapper classes, and the data type classes were converted.

The analysis toolbox is available on GitHub [\[10\]](#).

Bibliography

- [1] E. Adli and AWAKE Collaboration. [Towards Awake Applications: Electron Beam Acceleration in a Proton Driven Plasma Wake](#). In *Proceedings of IPAC 2016*, International Particle Accelerator Conference, pages 2557–2560, Busan, Korea, June 2016. JACoW. ISBN 978-3-95450-147-2. doi:[doi:10.18429/JACoW-IPAC2016-WEPMY008](https://doi.org/10.18429/JACoW-IPAC2016-WEPMY008).
- [2] E. Adli and P. Muggli. [Proton-Beam-Driven Plasma Acceleration](#). *Reviews of Accelerator Science and Technology*, 09:85–104, Jan. 2016. ISSN 1793-6268. doi:[10.1142/S1793626816300048](https://doi.org/10.1142/S1793626816300048).
- [3] E. Adli, V. K. Berglyd Olsen, C. A. Lindstrøm, P. Muggli, O. Reimann, J. M. Vieira, L. D. Amorim, C. I. Clarke, S. J. Gessner, S. Z. Green, M. J. Hogan, M. D. Litos, B. D. O'Shea, V. Yakimenko, C. Clayton, K. A. Marsh, W. B. Mori, C. Joshi, N. Vafaei-Najafabadi, and O. Williams. [Progress of plasma wakefield self-modulation experiments at FACET](#). *Nuclear Instruments and Methods in Physics Research Section A: Accelerators, Spectrometers, Detectors and Associated Equipment*, 829:334–338, Sept. 2016. ISSN 0168-9002. doi:[10.1016/j.nima.2016.02.075](https://doi.org/10.1016/j.nima.2016.02.075).
- [4] W. An, V. K. Decyk, W. B. Mori, and T. M. Antonsen. [An improved iteration loop for the three dimensional quasi-static particle-in-cell algorithm: QuickPIC](#). *Journal of Computational Physics*, 250:165–177, Oct. 2013. ISSN 0021-9991. doi:[10.1016/j.jcp.2013.05.020](https://doi.org/10.1016/j.jcp.2013.05.020).
- [5] S. Augst, D. Strickland, D. D. Meyerhofer, S. L. Chin, and J. H. Eberly. [Tunneling ionization of noble gases in a high-intensity laser field](#). *Physical Review Letters*, 63(20): 2212–2215, Nov. 1989. doi:[10.1103/PhysRevLett.63.2212](https://doi.org/10.1103/PhysRevLett.63.2212).
- [6] AWAKE Collaboration and A. Caldwell. [AWAKE Status Report, 2016](#). Technical Report CERN-SPSC-2016-033, CERN, Geneva, Switzerland, Oct. 2016.
- [7] AWAKE Collaboration and A. Caldwell. [AWAKE Status Report, 2017](#). Technical Report CERN-SPSC-2017-039, CERN, Geneva, Switzerland, Oct. 2017.
- [8] AWAKE Collaboration, R. Assmann, R. Bingham, T. Bohl, C. Bracco, B. Buttenschön, A. Butterworth, A. Caldwell, S. Chatopadhyay, S. Cipiccia, E. Feldbaumer, R. A. Fonseca, B. Goddard, M. Gross, O. Grulke, E. Gschwendtner, J. Holloway, C. Huang, D. Jaroszynski, S. Jolly, P. Kempkes, N. Lopes, K. Lotov, J. Machacek, S. R. Mandry, J. W. McKenzie, M. Meddahi, B. L. Militsyn, N. Moschuerling, P. Muggli, Z. Najmudin, T. C. Q. Noakes, P. A. Norreys, E. Öz, A. Pardons, A. Petrenko, A. Pukhov, K. Rieger, O. Reimann, H. Ruhl, E. Shaposhnikova, L. O. Silva, A. Sosedkin, R. Tarkeshian, R. M. G. N. Trines,

- T. Tückmantel, J. Vieira, H. Vincke, M. Wing, and G. Xia. [Proton-driven plasma wake-field acceleration: a path to the future of high-energy particle physics](#). *Plasma Physics and Controlled Fusion*, 56(8):084013, Aug. 2014. ISSN 0741-3335. doi:[10.1088/0741-3335/56/8/084013](https://doi.org/10.1088/0741-3335/56/8/084013).
- [9] V. K. Berglyd Olsen. [OsirisAnalysis: Matlab Analysis Code for Osiris Simulations](#). GitHub Repository, 2013. <https://github.com/vkbo/OsirisAnalysis>.
- [10] V. K. Berglyd Olsen. [QuickPICAnalysis: Matlab Analysis Code for QuickPIC Simulations](#). GitHub Repository, 2017. <https://github.com/vkbo/QuickPICAnalysis>.
- [11] V. K. Berglyd Olsen, E. Adli, P. Muggli, L. D. Amorim, and J. Vieira. [Loading of a Plasma-Wakefield Accelerator Section Driven by a Self-Modulated Proton Bunch](#). In *Proceedings of IPAC 2015*, pages 2551–2554, Richmond, VA, USA, May 2015. ISBN 978-3-95450-168-7. WEPWA026.
- [12] V. K. Berglyd Olsen, E. Adli, P. Muggli, and J. Vieira. [Loading of Wakefields in a Plasma Accelerator Section Driven by a Self-Modulated Proton Beam](#). In *Proceedings of NAPAC 2016*, North American Particle Accelerator Conference, Chicago, IL, USA, Oct. 2016. JACoW. ISBN 978-3-95450-180-9. doi:[10.18429/JACoW-NAPAC2016-TUA4CO03](https://doi.org/10.18429/JACoW-NAPAC2016-TUA4CO03). TUA4CO03.
- [13] V. K. Berglyd Olsen, J. J. Batkiewicz, S. Deghaye, S. J. Gessner, E. Gschwendtner, and P. Muggli. [Data Acquisition and Controls Integration of the AWAKE Experiment at CERN](#). In *Proceedings of IPAC 2017*, Copenhagen, Denmark, May 2017. JACoW. ISBN 978-3-95450-182-3. doi:[10.18429/JACoW-IPAC2017-TUPIK061](https://doi.org/10.18429/JACoW-IPAC2017-TUPIK061). TUPIK061.
- [14] V. K. Berglyd Olsen, E. Adli, and P. Muggli. [Emittance preservation of an electron beam in a loaded quasilinear plasma wakefield](#). *arXiv:1710.04858 [physics]*, Jan. 2018. arXiv: 1710.04858.
- [15] I. Blumenfeld, C. E. Clayton, F.-J. Decker, M. J. Hogan, C. Huang, R. Ischebeck, R. Iverson, C. Joshi, T. Katsouleas, N. Kirby, W. Lu, K. A. Marsh, W. B. Mori, P. Muggli, E. Oz, R. H. Siemann, D. Walz, and M. Zhou. [Energy doubling of 42 GeV electrons in a metre-scale plasma wakefield accelerator](#). *Nature*, 445(7129):741–744, Feb. 2007. ISSN 0028-0836. doi:[10.1038/nature05538](https://doi.org/10.1038/nature05538).
- [16] H. H. Braun, S. Döbert, I. Wilson, and W. Wuensch. [Frequency and Temperature Dependence of Electrical Breakdown at 21, 30, and 39 GHz](#). *Physical Review Letters*, 90(22): 224801, June 2003. doi:[10.1103/PhysRevLett.90.224801](https://doi.org/10.1103/PhysRevLett.90.224801).
- [17] A. Caldwell, K. Lotov, A. Pukhov, and F. Simon. [Proton-driven plasma-wakefield acceleration](#). *Nature Physics*, 5(5):363–367, May 2009. ISSN 1745-2473. doi:[10.1038/nphys1248](https://doi.org/10.1038/nphys1248).
- [18] A. Caldwell, E. Gschwendtner, K. Lotov, P. Muggli, and M. Wing. [AWAKE Status Report, 2015](#). Technical Report CERN-SPSC-2015-032. SPSC-SR-169, CERN, Geneva, Switzerland, Oct. 2015.

- [19] A. Caldwell, E. Adli, L. Amorim, R. ApSimon, T. Argyropoulos, R. Assmann, A. M. Bachmann, F. Batsch, J. Bauche, V. K. Berglyd Olsen, M. Bernardini, R. Bingham, B. Biskup, T. Bohl, C. Bracco, P. N. Burrows, G. Burt, B. Buttenschön, A. Butterworth, M. Cassella, S. Chattopadhyay, E. Chevallay, S. Cipiccia, H. Damerau, L. Deacon, P. Dirksen, S. Doeberl, U. Dorda, E. Elsen, J. Farmer, S. Fartoukh, V. Fedosseev, E. Feldbaumer, R. Fiorito, R. Fonseca, F. Friebel, G. Geschonke, B. Goddard, A. A. Gorn, O. Grulke, E. Gschwendtner, J. Hansen, C. Hessler, S. Hillenbrand, W. Hofle, J. Holloway, C. Huang, M. Hüther, D. Jaroszynski, L. Jensen, S. Jolly, A. Joulaei, M. Kasim, F. Keeble, R. Kersevan, N. Kumar, Y. Li, S. Liu, N. Lopes, K. V. Lotov, W. Lu, J. Machacek, S. Mandry, I. Martin, R. Martorelli, M. Martyanov, S. Mazzoni, M. Meddahi, L. Merminga, O. Mete, V. A. Minakov, J. Mitchell, J. Moody, A. S. Müller, Z. Najmudin, T. C. Q. Noakes, P. Norreys, J. Osterhoff, E. Öz, A. Pardons, K. Pepitone, A. Petrenko, G. Plyushchev, J. Pozimski, A. Pukhov, O. Reimann, K. Rieger, S. Roesler, H. Ruhl, T. Rusnak, F. Salveter, N. Savard, J. Schmidt, H. von der Schmitt, A. Seryi, E. Shaposhnikova, Z. M. Sheng, P. Sherwood, L. Silva, F. Simon, L. Soby, A. P. Sosedkin, R. I. Spitsyn, T. Tajima, R. Tarkeshian, H. Timko, R. Trines, T. Tückmantel, P. V. Tuev, M. Turner, F. Velotti, V. Verzilov, J. Vieira, H. Vincke, Y. Wei, C. P. Welsch, M. Wing, G. Xia, V. Yakimenko, H. Zhang, and F. Zimmermann. [Path to AWAKE: Evolution of the concept](#). *Nuclear Instruments and Methods in Physics Research Section A: Accelerators, Spectrometers, Detectors and Associated Equipment*, 829:3–16, Sept. 2016. ISSN 0168-9002. doi:[10.1016/j.nima.2015.12.050](https://doi.org/10.1016/j.nima.2015.12.050).
- [20] Y. W. Chan. [Ultra-intense laser radiation as a possible energy booster for relativistic charged particle](#). *Physics Letters A*, 35(4):305–306, June 1971. ISSN 0375-9601. doi:[10.1016/0375-9601\(71\)90397-5](https://doi.org/10.1016/0375-9601(71)90397-5).
- [21] F. F. Chen. *Introduction to Plasma Physics*. Springer, Boston, MA, 1974. ISBN 978-1-4757-0459-4. <https://doi.org/10.1007/978-1-4757-0459-4>.
- [22] P. Chen, J. M. Dawson, R. W. Huff, and T. Katsouleas. [Acceleration of Electrons by the Interaction of a Bunched Electron Beam with a Plasma](#). *Physical Review Letters*, 54(7):693–696, Feb. 1985. doi:[10.1103/PhysRevLett.54.693](https://doi.org/10.1103/PhysRevLett.54.693).
- [23] P. Chen, J. J. Su, T. Katsouleas, S. Wilks, and J. M. Dawson. [Plasma Focusing for High-Energy Beams](#). *IEEE Transactions on Plasma Science*, 15(2):218–225, Apr. 1987. ISSN 0093-3813. doi:[10.1109/TPS.1987.4316688](https://doi.org/10.1109/TPS.1987.4316688).
- [24] E. Chevallay, M. Csatari, A. Dabrowski, S. Doeberl, D. Egger, V. Fedosseev, Oznur Mete, M. Olvegaard, and M. Petrarca. [PHIN photo-injector as the CLIC drive beam source](#). *Journal of Physics: Conference Series*, 347(1):012036, 2012. ISSN 1742-6596. doi:[10.1088/1742-6596/347/1/012036](https://doi.org/10.1088/1742-6596/347/1/012036).
- [25] E. D. Courant and H. S. Snyder. [Theory of the alternating-gradient synchrotron](#). *Annals of Physics*, 3(1):1–48, Jan. 1958. ISSN 0003-4916. doi:[10.1016/0003-4916\(58\)90012-5](https://doi.org/10.1016/0003-4916(58)90012-5).
- [26] J. M. Dawson. [Nonlinear Electron Oscillations in a Cold Plasma](#). *Physical Review*, 113(2):383–387, Jan. 1959. doi:[10.1103/PhysRev.113.383](https://doi.org/10.1103/PhysRev.113.383).

- [27] E. Esarey, J. Krall, and P. Sprangle. Envelope analysis of intense laser pulse self-modulation in plasmas. *Physical Review Letters*, 72(18):2887–2890, May 1994. doi:[10.1103/PhysRevLett.72.2887](https://doi.org/10.1103/PhysRevLett.72.2887).
- [28] E. Esarey, P. Sprangle, J. Krall, and A. Ting. Overview of plasma-based accelerator concepts. *IEEE Transactions on Plasma Science*, 24(2):252–288, Apr. 1996. ISSN 0093-3813. doi:[10.1109/27.509991](https://doi.org/10.1109/27.509991).
- [29] R. A. Fonseca. Introduction to OSIRIS 4.0 for developers (and users). Presentation. OSIRIS Workshop 2017, 2017.
- [30] R. A. Fonseca, L. O. Silva, F. S. Tsung, V. K. Decyk, W. Lu, C. Ren, W. B. Mori, S. Deng, S. Lee, T. Katsouleas, and J. C. Adam. OSIRIS: A Three-Dimensional, Fully Relativistic Particle in Cell Code for Modeling Plasma Based Accelerators. In P. M. A. Sloot, A. G. Hoekstra, C. J. K. Tan, and J. J. Dongarra, editors, *Computational Science — ICCS 2002*, number 2331 in Lecture Notes in Computer Science, pages 342–351. Springer Berlin Heidelberg, 2002. ISBN 978-3-540-43594-5 978-3-540-47789-1. http://link.springer.com/chapter/10.1007/3-540-47789-6_36.
- [31] B. B. Godfrey. Numerical Cherenkov instabilities in electromagnetic particle codes. *Journal of Computational Physics*, 15(4):504–521, Aug. 1974. ISSN 0021-9991. doi:[10.1016/0021-9991\(74\)90076-X](https://doi.org/10.1016/0021-9991(74)90076-X).
- [32] A. D. Greenwood, K. L. Cartwright, J. W. Luginsland, and E. A. Baca. On the elimination of numerical Cerenkov radiation in PIC simulations. *Journal of Computational Physics*, 201(2):665–684, Dec. 2004. ISSN 0021-9991. doi:[10.1016/j.jcp.2004.06.021](https://doi.org/10.1016/j.jcp.2004.06.021).
- [33] E. Gschwendtner, K. Cornelis, I. Efthymiopoulos, A. Ferrari, A. Pardons, W. Treberspurg, H. Vincke, J. Wenninger, D. Autiero, A. Guglielmi, and P. Sala. Performance and Operational Experience of the CNGS Facility. In *Proceedings of IPAC 2010*, pages 4164–4166, Kyoto, Japan, May 2010. JACoW. ISBN 978-92-9083-352-9. THPEC046.
- [34] E. Gschwendtner, T. Bohl, C. Bracco, A. Butterworth, S. Cipiccia, S. Doeberl, V. Fedosseev, E. Feldbaumer, C. Hessler, W. Hofle, M. Martyanov, M. Meddahi, J. Osborne, A. Pardons, A. Petrenko, and H. Vincke. The AWAKE Experimental Facility at CERN. In *Proceedings of IPAC 2014*, pages 582–585, Dresden, Germany, 2014. JACoW. ISBN 978-3-95450-132-8. MOPRI005.
- [35] E. Gschwendtner, E. Adli, L. Amorim, R. Apsimon, R. Assmann, A. M. Bachmann, F. Batsch, J. Bauche, V. K. Berglyd Olsen, M. Bernardini, R. Bingham, B. Biskup, T. Bohl, C. Bracco, P. N. Burrows, G. Burt, B. Buttenschön, A. Butterworth, A. Caldwell, M. Cassella, E. Chevallay, S. Cipiccia, H. Damerau, L. Deacon, P. Dirksen, S. Doeberl, U. Dorda, J. Farmer, V. Fedosseev, E. Feldbaumer, R. Fiorito, R. Fonseca, F. Friebel, A. A. Gorn, O. Grulke, J. Hansen, C. Hessler, W. Hofle, J. Holloway, M. Hüther, D. Jaroszynski, L. Jensen, S. Jolly, A. Joulaei, M. Kasim, F. Keeble, Y. Li, S. Liu, N. Lopes, K. V. Lotov, S. Mandry, R. Martorelli, M. Martyanov, S. Mazzoni, O. Mete, V. A. Minakov, J. Mitchell, J. Moody, P. Muggli, Z. Najmudin, P. Norreys, E. Öz, A. Pardons, K. Pepitone,

- A. Petrenko, G. Plyushchev, A. Pukhov, K. Rieger, H. Ruhl, F. Salveter, N. Savard, J. Schmidt, A. Seryi, E. Shaposhnikova, Z. M. Sheng, P. Sherwood, L. Silva, L. Soby, A. P. Sosedkin, R. I. Spitsyn, R. Trines, P. V. Tuev, M. Turner, V. Verzilov, J. Vieira, H. Vincke, Y. Wei, C. P. Welsch, M. Wing, G. Xia, and H. Zhang. **AWAKE, The Advanced Proton Driven Plasma Wakefield Acceleration Experiment at CERN.** *Nuclear Instruments and Methods in Physics Research Section A*, 829:76–82, Sept. 2016. ISSN 0168-9002. doi:[10.1016/j.nima.2016.02.026](https://doi.org/10.1016/j.nima.2016.02.026).
- [36] M. J. Hogan. **Electron and Positron Beam–Driven Plasma Acceleration.** *Reviews of Accelerator Science and Technology*, 09:63–83, Jan. 2016. ISSN 1793-6268. doi:[10.1142/S1793626816300036](https://doi.org/10.1142/S1793626816300036).
- [37] C. Huang, V. K. Decyk, C. Ren, M. Zhou, W. Lu, W. B. Mori, J. H. Cooley, T. M. Antonsen, and T. Katsouleas. **QUICKPIC: A highly efficient particle-in-cell code for modeling wakefield acceleration in plasmas.** *Journal of Computational Physics*, 217(2):658–679, Sept. 2006. ISSN 0021-9991. doi:[10.1016/j.jcp.2006.01.039](https://doi.org/10.1016/j.jcp.2006.01.039).
- [38] E. Kallos, T. Katsouleas, W. D. Kimura, K. Kusche, P. Muggli, I. Pavlyshin, I. Pogorelsky, D. Stolyarov, and V. Yakimenko. **High-Gradient Plasma-Wakefield Acceleration with Two Subpicosecond Electron Bunches.** *Physical Review Letters*, 100(7):074802, Feb. 2008. doi:[10.1103/PhysRevLett.100.074802](https://doi.org/10.1103/PhysRevLett.100.074802).
- [39] T. Katsouleas, S. Wilks, P. Chen, J. M. Dawson, and J. J. Su. **Beam loading in plasma accelerators.** *Particle Accelerators*, 22(18):81–99, 1987.
- [40] J. Krall and G. Joyce. **Transverse equilibrium and stability of the primary beam in the plasma wake-field accelerator.** *Physics of Plasmas*, 2(4):1326–1331, Apr. 1995. ISSN 1070-664X. doi:[10.1063/1.871344](https://doi.org/10.1063/1.871344).
- [41] N. Kumar, A. Pukhov, and K. Lotov. **Self-Modulation Instability of a Long Proton Bunch in Plasmas.** *Physical Review Letters*, 104(25):255003, June 2010. doi:[10.1103/PhysRevLett.104.255003](https://doi.org/10.1103/PhysRevLett.104.255003).
- [42] E. P. Lee and R. K. Cooper. **General envelope equation for cylindrically symmetric charged-particle beams.** *Particle Accelerators*, 7(2):83–95, 1976.
- [43] S. Lee, T. Katsouleas, R. G. Hemker, E. S. Dodd, and W. B. Mori. **Plasma-wakefield acceleration of a positron beam.** *Physical Review E*, 64(4):045501, Sept. 2001. doi:[10.1103/PhysRevE.64.045501](https://doi.org/10.1103/PhysRevE.64.045501).
- [44] R. Lehe, A. Lifschitz, C. Thaury, V. Malka, and X. Davoine. **Numerical growth of emittance in simulations of laser-wakefield acceleration.** *Physical Review Special Topics - Accelerators and Beams*, 16(2):021301, Feb. 2013. doi:[10.1103/PhysRevSTAB.16.021301](https://doi.org/10.1103/PhysRevSTAB.16.021301).
- [45] M. Litos, E. Adli, W. An, C. I. Clarke, C. E. Clayton, S. Corde, J. P. Delahaye, R. J. England, A. S. Fisher, J. Frederico, S. Gessner, S. Z. Green, M. J. Hogan, C. Joshi, W. Lu, K. A. Marsh, W. B. Mori, P. Muggli, N. Vafaei-Najafabadi, D. Walz, G. White, Z. Wu, V. Yakimenko, and G. Yocky. **High-efficiency acceleration of an electron beam in**

a plasma wakefield accelerator. *Nature*, 515(7525):92–95, Nov. 2014. ISSN 0028-0836. doi:[10.1038/nature13882](https://doi.org/10.1038/nature13882).

- [46] W. Lu, C. Huang, M. M. Zhou, W. B. Mori, and T. Katsouleas. [Limits of linear plasma wakefield theory for electron or positron beams](#). *Physics of Plasmas*, 12(6):063101, May 2005. ISSN 1070-664X. doi:[10.1063/1.1905587](https://doi.org/10.1063/1.1905587).
- [47] W. Lu, C. Huang, M. Zhou, W. B. Mori, and T. Katsouleas. [Nonlinear Theory for Relativistic Plasma Wakefields in the Blowout Regime](#). *Physical Review Letters*, 96(16):165002, Apr. 2006. doi:[10.1103/PhysRevLett.96.165002](https://doi.org/10.1103/PhysRevLett.96.165002).
- [48] W. Lu, C. Huang, M. Zhou, M. Tzoufras, F. S. Tsung, W. B. Mori, and T. Katsouleas. [A nonlinear theory for multidimensional relativistic plasma wave wakefieldsa\)](#). *Physics of Plasmas (1994-present)*, 13(5):056709, May 2006. ISSN 1070-664X, 1089-7674. doi:[10.1063/1.2203364](https://doi.org/10.1063/1.2203364).
- [49] V. Malka and P. Mora. [Principles of laser–plasma accelerators](#). *Comptes Rendus Physique*, 10(2):106–115, Mar. 2009. ISSN 1631-0705. doi:[10.1016/j.crhy.2009.03.008](https://doi.org/10.1016/j.crhy.2009.03.008).
- [50] E. Mobs. [The CERN accelerator complex. Complexe des accélérateurs du CERN](#). Illustration. OPEN-PHO-ACCEL-2016-009, July 2016. <https://cds.cern.ch/record/2197559>.
- [51] A. Modena, Z. Najmudin, A. E. Dangor, C. E. Clayton, K. A. Marsh, C. Joshi, V. Malka, C. B. Darrow, C. Danson, D. Neely, and F. N. Walsh. [Electron acceleration from the breaking of relativistic plasma waves](#). *Nature*, 377(6550):377606a0, Oct. 1995. ISSN 1476-4687. doi:[10.1038/377606a0](https://doi.org/10.1038/377606a0).
- [52] P. Muggli. [Beam-driven, Plasma-based Particle Accelerators](#). In *CAS - CERN Accelerator School: Plasma Wake Acceleration*, pages 119–142, CERN, Geneva, Switzerland, May 2017. ISBN 978-92-9083-424-3. doi:[10.5170/CERN-2016-001.119](https://doi.org/10.5170/CERN-2016-001.119). arXiv: 1705.10537.
- [53] P. Muggli and M. J. Hogan. [Review of high-energy plasma wakefield experiments](#). *Comptes Rendus Physique*, 10(2):116–129, Mar. 2009. ISSN 1631-0705. doi:[10.1016/j.crhy.2009.03.004](https://doi.org/10.1016/j.crhy.2009.03.004).
- [54] P. Muggli, O. Reimann, E. Adli, V. Olsen, L. Amorim, S. Gessner, M. Hogan, S. Li, M. Litos, C. Joshi, K. Marsh, W. Mori, N. Vafaei-Najafabadi, N. Lopes, and J. Vieira. [Electron Bunch Self-modulation in Long Plasmas at SLAC FACET](#). In *Proceedings of IPAC 2014*, pages 1476–1478, Dresden, Germany, 2014. JACoW. ISBN 978-3-95450-132-8.
- [55] P. Muggli, E. Adli, R. Apsimon, F. Asmus, R. Baartman, A.-M. Bachmann, M. B. Marin, F. Batsch, J. Bauche, V. K. B. Olsen, M. Bernardini, B. Biskup, E. B. Vinuela, A. Boccardi, T. Bogey, T. Bohl, C. Bracco, F. Bra unmuller, S. Burger, G. Burt, S. Bustamante, B. Buttenschön, A. Butterworth, A. Caldwell, M. Casella, E. Chevallay, M. Chung, H. Damerau, L. Deacon, A. Dexter, P. Dirksen, S. Doeberl, J. Farmer, V. Fedosseev, T. Feniet, G. Fiori, R. Fiorito, R. Fonseca, F. Friebel, P. Gander, S. Gessner, I. Gorgisyan, A. A.

- Gorn, O. Grulke, E. Gschwendtner, A. Guerrero, J. Hansen, C. Hessler, W. Hofle, J. Hollaway, M. Hüther, M. Ibison, M. R. Islam, L. Jensen, S. Jolly, M. Kasim, F. Keeble, S.-Y. Kim, F. Kraus, A. Lasheen, T. Lefevre, G. LeGodec, Y. Li, S. Liu, N. Lopes, K. V. Lotov, M. Martyanov, S. Mazzoni, D. M. Godoy, O. Mete, V. A. Minakov, R. Mompo, J. Moody, M. T. Moreira, J. Mitchell, C. Mutin, P. Norreys, E. Öz, E. Ozturk, W. Pauw, A. Pardons, C. Pasquino, K. Pepitone, A. Petrenko, S. Pitmann, G. Plyushchev, A. Pukhov, K. Rieger, H. Ruhl, J. Schmidt, I. A. Shalimova, E. Shaposhnikova, P. Sherwood, L. Silva, A. P. Sosedkin, R. Speroni, R. I. Spitsyn, K. Szczurek, J. Thomas, P. V. Tuev, M. Turner, V. Verzilov, J. Vieira, H. Vincke, C. P. Welsch, B. Williamson, M. Wing, G. Xia, H. Zhang, and T. A. collaboration. [AWAKE readiness for the study of the seeded self-modulation of a 400 GeV proton bunch](#). *Plasma Physics and Controlled Fusion*, 60(1):014046, Nov. 2017. ISSN 0741-3335. doi:[10.1088/1361-6587/aa941c](https://doi.org/10.1088/1361-6587/aa941c).
- [56] E. Öz, F. Batsch, and P. Muggli. [An accurate Rb density measurement method for a plasma wakefield accelerator experiment using a novel Rb reservoir](#). *Nuclear Instruments and Methods in Physics Research Section A: Accelerators, Spectrometers, Detectors and Associated Equipment*, 829:321–325, Sept. 2016. ISSN 01689002. doi:[10.1016/j.nima.2016.02.005](https://doi.org/10.1016/j.nima.2016.02.005). arXiv: 1511.08763.
- [57] R. B. Palmer. [Interaction of Relativistic Particles and Free Electromagnetic Waves in the Presence of a Static Helical Magnet](#). *Journal of Applied Physics*, 43(7):3014–3023, July 1972. ISSN 0021-8979. doi:[10.1063/1.1661650](https://doi.org/10.1063/1.1661650).
- [58] H. L. Pécseli. *Waves and Oscillations in Plasmas*. CRC Press, Boca Raton, 1st edition, Sept. 2012. ISBN 978-1-4398-7848-4.
- [59] K. Pepitone, S. Doeberl, G. Burt, E. Chevallay, N. Chritin, C. Delory, V. Fedossev, C. Hessler, G. McMonagle, O. Mete, V. Verzilov, and R. Apsimon. [The electron accelerator for the AWAKE experiment at CERN](#). *Nuclear Instruments and Methods in Physics Research Section A: Accelerators, Spectrometers, Detectors and Associated Equipment*, 829(Supplement C):73–75, Sept. 2016. ISSN 0168-9002. doi:[10.1016/j.nima.2016.02.025](https://doi.org/10.1016/j.nima.2016.02.025).
- [60] D. P. Pritchau and R. H. Siemann. [Experimental Study of RF Pulsed Heating on Oxygen Free Electronic Copper](#). *Physical Review Special Topics - Accelerators and Beams*, 5(11):112002, Nov. 2002. doi:[10.1103/PhysRevSTAB.5.112002](https://doi.org/10.1103/PhysRevSTAB.5.112002).
- [61] A. Pukhov and J. Meyer-ter Vehn. [Laser wake field acceleration: the highly non-linear broken-wave regime](#). *Applied Physics B*, 74(4-5):355–361, Apr. 2002. ISSN 0946-2171, 1432-0649. doi:[10.1007/s003400200795](https://doi.org/10.1007/s003400200795).
- [62] K. Rieger, A. Caldwell, O. Reimann, and P. Muggli. [GHz modulation detection using a streak camera: Suitability of streak cameras in the AWAKE experiment](#). *Review of Scientific Instruments*, 88(2):025110, Feb. 2017. ISSN 0034-6748. doi:[10.1063/1.4975380](https://doi.org/10.1063/1.4975380).
- [63] J. B. Rosenzweig, D. B. Cline, B. Cole, H. Figueroa, W. Gai, R. Konecny, J. Norem, P. Schoessow, and J. Simpson. [Experimental Observation of Plasma Wake-Field Acceleration](#). *Physical Review Letters*, 61(1):98–101, July 1988. doi:[10.1103/PhysRevLett.61.98](https://doi.org/10.1103/PhysRevLett.61.98).

- [64] F. Salin, P. Georges, G. Roger, and A. Brun. [Single-shot measurement of a 52-fs pulse](#). *Applied Optics*, 26(21):4528–4531, Nov. 1987. ISSN 1539-4522. doi:[10.1364/AO.26.004528](https://doi.org/10.1364/AO.26.004528).
- [65] K. Schindl. [Space charge](#). In *Proceedings of the Joint US–CERN–Japan–Russia School on Particle Accelerators*, pages 127–151, Montreux and CERN, Switzerland, May 1999. World Scientific. ISBN 978-981-02-3881-0. doi:[10.1142/9789812818003_0004](https://doi.org/10.1142/9789812818003_0004).
- [66] A. Schwinn, S. Matthies, D. Pfeiffer, M. Arruat, L. Fernandez, F. Locci, and D. G. Saavedra. [FESA3 – The New Front-End Software Framework at CERN and the FAIR Facility](#). In *Proceedings of PCaPAC 2010*, pages 22–26, Saskatoon, Saskatchewan, Canada, 2010. JACoW. ISBN 978-1-63266-483-9. WECOAA03.
- [67] T. Tajima and J. M. Dawson. [Laser Electron Accelerator](#). *Physical Review Letters*, 43(4):267–270, July 1979. doi:[10.1103/PhysRevLett.43.267](https://doi.org/10.1103/PhysRevLett.43.267).
- [68] L. Tonks and I. Langmuir. [Oscillations in Ionized Gases](#). *Physical Review*, 33(2):195–210, Feb. 1929. doi:[10.1103/PhysRev.33.195](https://doi.org/10.1103/PhysRev.33.195).
- [69] UCLA Plasma Simulation Group. [QuickPIC-OpenSource](#). repository. GitHub repository, 2017. <https://github.com/UCLA-Plasma-Simulation-Group/QuickPIC-OpenSource>.
- [70] J. Vieira, R. A. Fonseca, W. B. Mori, and L. O. Silva. [Ion Motion in Self-Modulated Plasma Wakefield Accelerators](#). *Physical Review Letters*, 109(14):145005, Oct. 2012. doi:[10.1103/PhysRevLett.109.145005](https://doi.org/10.1103/PhysRevLett.109.145005).
- [71] J. Vieira, L. D. Amorim, Y. Fang, W. B. Mori, P. Muggli, and L. O. Silva. [Self-modulation instability of ultra-relativistic particle bunches with finite rise times](#). *Plasma Physics and Controlled Fusion*, 56(8):084014, 2014. ISSN 0741-3335. doi:[10.1088/0741-3335/56/8/084014](https://doi.org/10.1088/0741-3335/56/8/084014).
- [72] K. Wille. *The Physics of Particle Accelerators: An Introduction*. Clarendon Press, Oxford, New York, first edition, May 2001. ISBN 978-0-19-850549-5.
- [73] K. Yee. Numerical solution of initial boundary value problems involving maxwell's equations in isotropic media. *IEEE Transactions on Antennas and Propagation*, 14(3):302–307, May 1966. ISSN 0018-926X. doi:[10.1109/TAP.1966.1138693](https://doi.org/10.1109/TAP.1966.1138693).